

EFFECTIVE PROPERTIES OF THREE-PHASE ELECTRO-MAGNETO-ELASTIC
MULTIFUNCTIONAL COMPOSITE MATERIALS

A Thesis

by

JAE SANG LEE

Submitted to the Office of Graduate Studies of
Texas A&M University
in partial fulfillment of the requirements for the degree of

MASTER OF SCIENCE

December 2003

Major Subject: Aerospace Engineering

EFFECTIVE PROPERTIES OF THREE-PHASE ELECTRO-MAGNETO-ELASTIC
MULTIFUNCTIONAL COMPOSITE MATERIALS

A Thesis

by

JAE SANG LEE

Submitted to Texas A&M University
in partial fulfillment of the requirements
for the degree of

MASTER OF SCIENCE

Approved as to style and content by:

Dimitris C. Lagoudas
(Chair of Committee)

James G. Boyd IV
(Member)

Roger Morgan
(Member)

Walter E Haisler
(Head of Department)

December 2003

Major Subject: Aerospace Engineering

ABSTRACT

Effective Properties of Three-Phase Electro-Magneto-Elastic
Multifunctional Composite Materials. (December 2003)

Jae Sang Lee, B.S., Seoul National University, Seoul, Korea

Chair of Advisory Committee: Dr. Dimitris C. Lagoudas

Coupling between the electric field, magnetic field, and strain of composite materials is achieved when electro-elastic (piezoelectric) and magneto-elastic (piezomagnetic) particles are joined by an elastic matrix. Although the matrix is neither piezoelectric nor piezomagnetic, the strain field in the matrix couples the \mathbf{E} field of the piezoelectric phase to the \mathbf{B} field of the piezomagnetic phase. This three-phase electro-magneto-elastic composite should have greater ductility and formability than a two-phase composite in which \mathbf{E} and \mathbf{B} are coupled by directly bonding two ceramic materials with no compliant matrix. A finite element analysis and homogenization of a representative volume element is performed to determine the effective electric, magnetic, mechanical, and coupled-field properties of an elastic (epoxy) matrix reinforced with piezoelectric and piezomagnetic fibers as functions of the phase volume fractions, the fiber (or particle) shapes, the fiber arrangements in the unit cell, and the fiber material properties with special emphasis on the symmetry properties of the fibers and the poling directions of the piezoelectric and piezomagnetic fibers. The effective magnetoelectric moduli of this three-phase composite are, however, less than the

effective magnetoelectric coefficients of a two-phase piezoelectric/piezomagnetic composite, because the epoxy matrix is not stiff enough to transfer significant strains between the piezomagnetic and piezoelectric fibers.

To my parents, sisters, friends, JIVE and allornon.

TABLE OF CONTENTS

	Page
ABSTRACT	iii
DEDICATION	v
TABLE OF CONTENTS	vi
LIST OF FIGURES.....	viii
LIST OF TABLES	xi
CHAPTER	
I INTRODUCTION.....	1
A. Literature Review.....	1
B. Motivation.....	4
C. Three-phase Electro-magneto-elastic Composite	5
D. Femlab.....	5
E. Scope of the Thesis.....	6
II THREE-PHASE ELECTRO-MAGNETO-ELASTIC COMPOSITE	7
A. Three-phase Electro-magneto-elastic Composite	7
B. Basic Equations.....	7
1. Constituent phases.....	7
2. Effective electro-magneto-elastic composite	9
III MICROMECHANICAL APPROACH	11
A. The Effective Properties of N-phase Composites.....	11
B. Mori-Tanaka Method for Three-phase Electro-magneto-elastic Composite	13

CHAPTER	Page
IV	FINITE ELEMENT METHOD..... 15
	A. Periodic Unit Cell 15
	B. Periodic Boundary Conditions 15
	C. Evaluation of the Effective Constitutive Equations 18
	D. Element and Solver 19
V	RESULTS AND DISCUSSION..... 20
	A. Two-phase Electro-magneto-elastic Composite 20
	B. Three-phase Electro-magneto-elastic Composite 27
	C. Parametric Studies..... 32
	1. Effects of volume fractions 33
	a. Fixed elastic matrix volume fraction 33
	b. Fixed piezoelectric and piezomagnetic volume ratio 36
	2. Effects of poling direction 39
VI	CONCLUSIONS 45
	REFERENCES 47
	APPENDIX A 51
	APPENDIX B 52
	APPENDIX C 55
	APPENDIX D 57
	VITA 89

LIST OF FIGURES

FIGURE	Page
1 Three-phase electro-magneto-elastic composite	7
2 Periodic structure model and Periodic unit cell	15
3 Schematic of the periodic unit cell used for the periodic boundary conditions	16
4 Mesh shape of two-phase composite and three-phase composite	19
5 Square unit cell and hexagonal unit cell.....	21
6 C_{11} distribution for rotational variation of a two-phase composite	23
7 C_{12} distribution for rotational variation of a two-phase composite	24
8 C_{66} distribution for rotational variation of a two-phase composite	24
9 Difference distribution for rotational variation for a two-phase composite.....	25
10 The unit cell of a fibrous two-phase composite	26
11 Effective elastic moduli of a fibrous two-phase composite vs v_f	26
12 Effective dielectric moduli of a fibrous two-phase composite vs v_f	26
13 Effective magnetic moduli of a fibrous two-phase composite vs v_f	26
14 Effective piezoelectric moduli of a fibrous two-phase composite vs v_f	26
15 Effective piezomagnetic moduli of a fibrous two-phase composite vs v_f	26
16 Effective magnetoelectric constant λ_{33} of a fibrous two-phase composite vs v_f	26
17 Electric potential distribution of a fibrous three-phase electro-magneto-elastic composite when $\langle E_1 \rangle$ is applied.....	28
18 Electric field E_1 distribution of a fibrous three-phase electro-magneto-elastic	

FIGURE	Page
composite when $\langle E_1 \rangle$ is applied	28
19 Shear strain ε_{31} distribution of a fibrous three-phase electro-magneto-elastic composite when $\langle E_1 \rangle$ is applied.....	29
20 Magnetic field H_1 distribution of a fibrous three-phase electro-magneto-elastic composite when $\langle E_1 \rangle$ is applied.....	29
21 Magnetic potential distribution of a fibrous three-phase electro-magneto-elastic composite when $\langle E_1 \rangle$ is applied.....	29
22 C_{11} distribution for rotational variation of a three-phase composite	31
23 C_{12} distribution for rotational variation of a three-phase composite	31
24 C_{66} distribution for rotational variation of a three-phase composite	32
25 Difference distribution for rotational variation for a two-phase composite.....	32
26 Effective stiffness C_{11} vs ν_f	34
27 Effective stiffness C_{12} vs ν_f	34
28 Effective stiffness C_{13} vs ν_f	35
29 Effective stiffness C_{33} vs ν_f	35
30 Effective stiffness C_{44} vs ν_f	35
31 Effective stiffness C_{66} vs ν_f	35
32 Effective piezoelectric constants vs ν_f	35
33 Effective piezomagnetic constants vs ν_f	35
34 Effective dielectric permittivity vs ν_f	36
35 Effective magnetic permeability vs ν_f	36

FIGURE	Page
36 Effective magnetoelectric constant λ_{11} vs ν_f	36
37 Effective magnetoelectric constant λ_{33} vs ν_f	36
38 Effective stiffness C_{11} vs ν_m	37
39 Effective stiffness C_{12} vs ν_m	37
40 Effective stiffness C_{13} vs ν_m	38
41 Effective stiffness C_{33} vs ν_m	38
42 Effective stiffness C_{44} vs ν_m	38
43 Effective stiffness C_{66} vs ν_m	38
44 Effective piezoelectric constants vs ν_m	38
45 Effective piezomagnetic constants vs ν_m	38
46 Effective dielectric permittivity vs ν_m	39
47 Effective magnetic permeability vs ν_m	39
48 Effective magnetoelectric constant λ_{11} vs ν_m	39
49 Effective magnetoelectric constant λ_{33} vs ν_m	39

LIST OF TABLES

TABLE	Page
1 Boundary condition equations.....	17
2 Material properties of $BaTiO_3$ and $CoFe_2O_4$	27
3 Poling direction of each case.....	40

CHAPTER I

INTRODUCTION

A. Literature Review

Efforts are currently under way to develop materials that have superior properties to those currently existing. This has resulted in the development of composite materials that exhibit remarkable product properties, which are created by the interaction between the constituent phases. There are many advantages to using composite materials over more traditional materials, such as the possibility of weight or volume reduction in a structure while maintaining a comparable or improved performance level [1]. Pyroelectricity, which is achieved by combining a material with a large thermal expansion coefficient with a piezoelectric material, is used in numerous thermal-imaging devices and sensors. The composite can exhibit pyroelectricity even though neither of the constituents does [2]. The magnetoelectric coupling effect in composite materials consisting of a piezoelectric phase and a piezomagnetic phase has recently attracted attention due to the extensive applications for broadband magnetic field probes, electric packaging, acoustic, hydrophones, medical ultrasonic imaging, sensors, and actuators [3, 4, 5, 6, 7]. These composites are regarded as *smart* or *intelligent* materials. The analytical modeling of such composites provides the opportunity to study the effect of controlling and altering the response of composite structures that consist of composite materials [8].

This thesis follows the style and format of *IEEE Transactions on Automatic Control*.

In 1974 Van Run et al. (1974) reported that the magnetoelectric effect obtained in a $BaTiO_3 - CoFeO_4$ composite was two orders of magnitude larger than that of the single-phase magnetoelectric material Co_2O_3 [9]. Bracke and Van Vliet (1981) reported a broad band magnetoelectric transducer with a flat frequency response using composite materials. Since then, much of the theoretical and experimental work for investigation into the magnetoelectric coupling effect has been carried out in papers published by Harshe (1991), Harshe et al. (1993), Avellaneda and Harshe (1994), Nan (1994), Benveniste (1995), Huang and Kuo (1997), Li and Dunn (1998), Wu and Huang (2000) and Aboudi (2001). They obtained expressions for the effective magnetoelectric coefficient and a figure of merit for magnetoelectric coupling.

Harshe, Dougherty, and Newnham (1993) treated magnetoelectric effect of piezoelectric-piezomagnetic composites in terms of a simple approach. They assumed a relatively simple geometrical model, a cubes model, in which the so-called 0-3 or 3-0 composite with particles of one phase (denoted by 0) embedded in the matrix of the second phase (denoted by 3) was considered as consisting of small cubes. Then, they solved the fields in one cube for which the boundary value problem involved is tractable. This simple cubes model is an elementary series-parallel-like model and is lacking in theoretical rigor [10, 11].

Nan (1994) proposed a theoretical framework based on a Green's function method and perturbation theory, which have been widely employed to treat the general, linear-response properties of inhomogeneous media [10]. However, Benveniste (1995) derived exact connections between the effective moduli of piezoelectric-piezomagnetic

two-phase composites, which were independent of the details of the microgeometry and of the particular choice of the averaging model, using the uniform field concept [12, 13]. The so-called non-self-consistency approximation (NSC) of Nan failed to satisfy the exact connections between different components of the effective moduli obtained by Benveniste.

Li and Dunn (1998) developed a micromechanics approach to analyze the average fields and effective moduli for two phase piezoelectric-piezomagnetic composites [1]. They derived explicit expressions for the generalized Eshelby tensors, which are used for micromechanics modeling of heterogeneous solids and exact relations regarding the effective behavior and the average fields. Then Li and Dunn obtained the closed form expressions for the effective moduli of two-phase composites as well as the exact connections between the effective thermal moduli and the effective electro-magneto-elastic moduli of two-phase composites applying the Mori-Tanaka mean field approach.

The Mori-Tanaka method was also employed by Wu and Huang (2000) in order to obtain the electro-magneto-elastic Eshelby tensors and the effective material properties of piezoelectric-piezomagnetic composites [14]. By taking the derivative of the closed form for magnetoelectric coupling effect with respect to the fiber volume fraction as zeros, Huang et al (2000) obtained the optimized volume fraction of fibers analytically and showed that the magnetoelectric coupling effect is a function of the elastic properties of constituents, but not a function of the magnetic and electric properties [15].

Li (2000) generalized the Mori-Tanaka theorem and Nemat-Nasser and Hori's multi-inclusion model to analyze the heterogeneous electro-magneto-elastic solids. His analysis served as a basis for an averaging scheme to determine the effective electro-magneto-elastic moduli of composite materials.

Aboudi (2001) employed a homogenization micromechanical method for the prediction of the effective moduli of electro-magneto-thermo-elastic multiphase composites [8]. The homogenization method assumes that fields vary on multiple spatial scales due to the existence of a microstructure and that the microstructure is spatially periodic. It was seen that the homogenization theory and Mori-Tanaka results of Li and Dunn (1998) were very similar. To date, the micromechanics of magnetoelectric composites have focused on two-phase composites.

B. Motivation

Unfortunately, piezoelectric and piezomagnetic materials are usually brittle ceramics, therefore the composite consisting of those two phases would be susceptible to brittle fracture. Thus, the third phase, the elastic phase, is introduced to increase the ductility. A three-phase electro-magneto-elastic composite consisting of piezoelectric and piezomagnetic phases separated by a polymer matrix would have greater ductility and formability. Recently, Boyd et al (2001) presented a method for using arrays of MEMS (Micro-Electro-Mechanical Systems) electrodes and electromagnets to achieve microscale positioning of piezoelectric and piezomagnetic particles in liquid polymers, which would then be solidified to make a polymer matrix magnetoelectric composite [16]. The ability to pattern the particles into microscale unit cells would reduce

concentrations of stress, electric field, and magnetic field, thereby increasing effective threshold properties such as strength, electric breakdown field, and magnetic saturation field. Furthermore, one can hope that someday arrays of MEMS can be used to control the microscale distribution of the poling direction of piezoelectric and piezomagnetic particles.

C. Three-phase Electro-magneto-elastic Composite

Motivated by the work of Boyd et al (2001), in the present paper we calculate the effective magnetoelectric coefficients of three-phase composites consisting of piezoelectric and piezomagnetic phases separated by an elastic matrix. Although the matrix is neither piezoelectric nor piezomagnetic, the strain field in the matrix couples the E field of the piezoelectric phase to the B field of the piezomagnetic phase. The finite element method is used because, unlike closed-form micromechanics methods, the finite element method reveals the concentration of stress, electric field, and magnetic field within the unit cell. These field concentrations determine the effective strength, electric breakdown field, and magnetic saturation field of the composite. Homogenization is then applied on the FEA (Finite Element Analysis) solution for the average (effective) electro-magneto-elastic properties.

D. Femlab

Commercially available software known as FEMLAB is employed in the computational analysis. FEMLAB is a program that supports the equation based modeling, which means that the software does not need the differential equations to be

solved in advance. The user may supply any desired system of differential equations and the software generates the appropriate FEM (Finite Element Method) formulation. This is very useful in solving multi-physics problems in which one may have significant coupling of variables. The appropriate partial differential equations for each sub-domain are given as input, and the corresponding appropriate boundary condition equations and specific boundary values are input as well.

E. Scope of the Thesis

The basic equations and notation used for each phase are presented in Chapter II. The mean-field theory for three-phase electro-magneto-electric composites and the finite element and homogenization method of a unit cell are presented in Chapter III and Chapter IV, respectively. In section A of Chapter V, the results of a finite element analysis are compared to the Mori-Tanaka results of Li and Dunn (1998) for a two-phase composite consisting of a piezomagnetic matrix with piezoelectric fibers. For a three-phase composite, the finite element results are presented in section B. In section C, the parametric studies are presented with special emphasis on the phase volume fraction and the poling directions of the piezoelectric and piezomagnetic fibers.

CHAPTER II

THREE-PHASE ELECTRO-MAGNETO-ELASTIC COMPOSITE

A. Three-phase Electro-magneto-elastic Composite

Consider a composite material with cylindrical piezoelectric and piezomagnetic fibers aligned periodically as shown in Figure 1. The piezoelectric and piezomagnetic fibers are transversely isotropic and the elastic matrix is isotropic. The matrix and fibers are assumed to be perfectly bonded without any sliding, void nucleation, or growth on their interfaces.

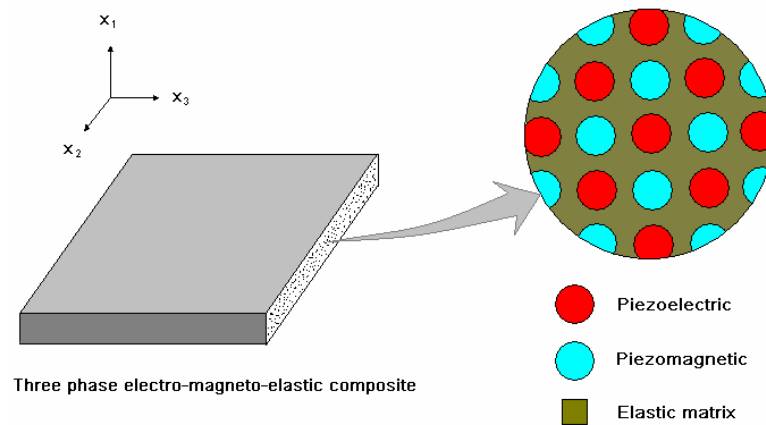


Figure 1. Three-phase electro-magneto-elastic composite

B. Basic Equations

1. Constituent phases

In order to assess the three-phase electro-magneto-elastic composite response, the framework of the model is introduced. For the piezoelectric phase, the piezomagnetic

phase, and elastic matrix, the constitutive equations are given in Equations (1a-c) below respectively:

$$\begin{array}{lll}
 \boldsymbol{\sigma} = \mathbf{C}\boldsymbol{\varepsilon} - \mathbf{e}^T \mathbf{E} & \boldsymbol{\sigma} = \mathbf{C}\boldsymbol{\varepsilon} - \mathbf{q}^T \mathbf{H} & \boldsymbol{\sigma} = \mathbf{C}\boldsymbol{\varepsilon} \\
 \mathbf{D} = \mathbf{e}\boldsymbol{\varepsilon} + \boldsymbol{\eta}\mathbf{E} & \mathbf{D} = \boldsymbol{\eta}\mathbf{E} & \mathbf{D} = \boldsymbol{\eta}\mathbf{E} \\
 \mathbf{B} = \boldsymbol{\mu}\mathbf{H} & \mathbf{B} = \mathbf{q}\boldsymbol{\varepsilon} + \boldsymbol{\mu}\mathbf{H} & \mathbf{B} = \boldsymbol{\mu}\mathbf{H}
 \end{array} \quad (1a-c)$$

where $\boldsymbol{\sigma}$, $\boldsymbol{\varepsilon}$, \mathbf{C} , $\boldsymbol{\eta}$, $\boldsymbol{\mu}$, \mathbf{e} and \mathbf{q} are the stress, strain, elastic stiffness, dielectric permittivity, magnetic permeability, piezoelectric coefficient, and piezomagnetic coefficient tensors. \mathbf{D} , \mathbf{E} , \mathbf{B} and \mathbf{H} are the electric displacement, electric field, magnetic flux and magnetic field vectors. The various constitutive coefficient tensors, which are assumed to exhibit transverse isotropy with x_3 as a symmetry axis, are given by the following explicit expressions:

$$\mathbf{C} = \begin{pmatrix} C_{11} & C_{12} & C_{13} & 0 & 0 & 0 \\ C_{12} & C_{11} & C_{13} & 0 & 0 & 0 \\ C_{13} & C_{13} & C_{33} & 0 & 0 & 0 \\ 0 & 0 & 0 & C_{44} & 0 & 0 \\ 0 & 0 & 0 & 0 & C_{44} & 0 \\ 0 & 0 & 0 & 0 & 0 & \frac{1}{2}(C_{11} - C_{12}) \end{pmatrix} \quad \mathbf{e} = \begin{pmatrix} 0 & 0 & 0 & 0 & e_{15} & 0 \\ 0 & 0 & 0 & e_{15} & 0 & 0 \\ e_{31} & e_{31} & e_{33} & 0 & 0 & 0 \end{pmatrix} \quad (2a-b)$$

$$\mathbf{q} = \begin{pmatrix} 0 & 0 & 0 & 0 & q_{15} & 0 \\ 0 & 0 & 0 & q_{15} & 0 & 0 \\ q_{31} & q_{31} & q_{33} & 0 & 0 & 0 \end{pmatrix} \quad \boldsymbol{\eta} = \begin{pmatrix} \eta_{11} & 0 & 0 \\ 0 & \eta_{11} & 0 \\ 0 & 0 & \eta_{33} \end{pmatrix} \quad \boldsymbol{\mu} = \begin{pmatrix} \mu_{11} & 0 & 0 \\ 0 & \mu_{11} & 0 \\ 0 & 0 & \mu_{33} \end{pmatrix} \quad (2c-e)$$

The balance of linear momentum (quasi-static conditions), Gauss' law, and the conservation of magnetic flux (no magnetic charges) are given by

$$\nabla \cdot \boldsymbol{\sigma} = 0, \quad \nabla \cdot \mathbf{D} = 0, \quad \nabla \cdot \mathbf{B} = 0 \quad (3a-c)$$

By the theory of electrostatics and magnetostatics, the electric field \mathbf{E} and the magnetic field strength \mathbf{H} are the gradient of an electric potential ϕ and a magnetic potential Φ :

$$\mathbf{E} = -\nabla\phi, \quad \mathbf{H} = -\nabla\Phi \quad (4a-b)$$

We assume small displacement gradient and employ the linearized strain-displacement relations are given by

$$\boldsymbol{\varepsilon} = \frac{1}{2}(\nabla\mathbf{u} + (\nabla\mathbf{u})^T) \quad (5)$$

Combining governing differential equations (2)-(5) with the constitutive equations (1a-c) results in the following field equations (6a-c) for u_1, u_2, u_3, ϕ and Φ in the piezoelectric, piezomagnetic and elastic phases respectively:

$$\begin{aligned} \nabla \cdot (\mathbf{C}\nabla\mathbf{u} + \mathbf{e}^T\nabla\phi) &= 0 & \nabla \cdot (\mathbf{C}\nabla\mathbf{u} + \mathbf{q}^T\nabla\Phi) &= 0 & \nabla \cdot (\mathbf{C}\nabla\mathbf{u}) &= 0 \\ \nabla \cdot (\mathbf{e}\nabla\mathbf{u} - \boldsymbol{\eta}\nabla\phi) &= 0 & \nabla \cdot (-\boldsymbol{\eta}\nabla\phi) &= 0 & \nabla \cdot (-\boldsymbol{\eta}\nabla\phi) &= 0 & (6a) \quad (6b) \quad (6c) \\ \nabla \cdot (-\boldsymbol{\mu}\nabla\Phi) &= 0 & \nabla \cdot (\mathbf{q}\nabla\mathbf{u} - \boldsymbol{\mu}\nabla\Phi) &= 0 & \nabla \cdot (-\boldsymbol{\mu}\nabla\Phi) &= 0 \end{aligned}$$

These field equations are implemented in the FEM and solved for a boundary value problem having periodic boundary conditions. The field equations for the constituent phases of the three-phase electro-magneto-elastic composite with x_3 as a symmetry axis are shown in Appendix A.

2. Effective electro-magneto-elastic composite

We consider electro-magneto-elastic media that exhibit linear, static, anisotropic coupling between the magnetic, electric, and elastic fields. In this case, the constitutive equations can be expressed as

$$\begin{aligned}
\boldsymbol{\sigma} &= \mathbf{C}\boldsymbol{\varepsilon} - \mathbf{e}^T \mathbf{E} - \mathbf{q}^T \mathbf{H} \\
\mathbf{D} &= \mathbf{e}\boldsymbol{\varepsilon} + \boldsymbol{\eta} \mathbf{E} + \boldsymbol{\lambda} \mathbf{H} \\
\mathbf{B} &= \mathbf{q}\boldsymbol{\varepsilon} + \boldsymbol{\lambda}^T \mathbf{E} + \boldsymbol{\mu} \mathbf{H}
\end{aligned} \tag{7}$$

where $\boldsymbol{\lambda}$ is the (3x3) magnetoelectric coefficient tensor.

The effective constitutive coefficient tensors of the composite are defined in terms of averaged fields. This is based on the fact that the effective properties of a composite are relations between the volume average of the strain, electric field, magnetic field, stress, electric density and magnetic flux of microscopically heterogeneous media. Field variables over the entire boundary can be averaged to obtain effective constitutive response as

$$\begin{aligned}
\langle \boldsymbol{\sigma} \rangle &= \mathbf{C}^* \langle \boldsymbol{\varepsilon} \rangle - \mathbf{e}^{T*} \langle \mathbf{E} \rangle - \mathbf{q}^{T*} \langle \mathbf{H} \rangle \\
\langle \mathbf{D} \rangle &= \mathbf{e}^* \langle \boldsymbol{\varepsilon} \rangle + \boldsymbol{\eta}^* \langle \mathbf{E} \rangle + \boldsymbol{\lambda}^* \langle \mathbf{H} \rangle \\
\langle \mathbf{B} \rangle &= \mathbf{q}^* \langle \boldsymbol{\varepsilon} \rangle + \boldsymbol{\lambda}^{T*} \langle \mathbf{E} \rangle + \boldsymbol{\mu}^* \langle \mathbf{H} \rangle
\end{aligned} \tag{8}$$

The brackets denote the volume average, $\langle \bullet \rangle = \frac{1}{V} \int \bullet dV$, where V is the volume of representative volume element. Although $\boldsymbol{\lambda}$ is absent in each of the phases within the representative volume element, the effective properties of the composite may contain a non-zero magnetoelectric coefficient because the magnetic and electric fields of the piezomagnetic and piezoelectric particles are coupled through the matrix strain field.

CHAPTER III

MICROMECHANICAL APPROACH

In this chapter, the generalized expression for the effective properties of N-phase electro-magneto-elastic composites and the Mori-Tanaka theory for the three-phase electro-magneto-elastic composites which is used for comparison with FEA are introduced. The matrix and the dispersed phase are assumed to be perfectly bonded without any sliding, void nucleation, or growth on their interfaces.

A. The Effective Properties of N-phase Composites

Consider a heterogeneous composite material consisting of an elastic matrix with cylindrical piezoelectric and piezomagnetic fibrous inclusions aligned along x_3 axis. We require that the material properties of the dispersed phase are constant with respect to a fixed coordinate system. Thus, orientational variations of an anisotropic dispersed phase are prohibited [1]. To treat the elastic, electric and magnetic variables on equal footing, the constitutive relations are compactly expressed in the following notation.

$$\begin{pmatrix} \boldsymbol{\sigma} \\ \mathbf{D} \\ \mathbf{B} \end{pmatrix} = \begin{pmatrix} \mathbf{C} & \mathbf{e}^T & \mathbf{q}^T \\ \mathbf{e} & -\boldsymbol{\eta} & \boldsymbol{\lambda}^T \\ \mathbf{q} & \boldsymbol{\lambda} & -\boldsymbol{\mu} \end{pmatrix} \begin{pmatrix} \boldsymbol{\varepsilon} \\ -\mathbf{E} \\ -\mathbf{H} \end{pmatrix} \Leftrightarrow \boldsymbol{\Sigma} = \mathbf{LZ} \quad (9)$$

Consider that the heterogeneous composite material is subjected to homogeneous potential boundary conditions \mathbf{Z}^o , meaning that, when they are applied to a homogeneous solid, they result in homogeneous fields. The average strain theorem of elasticity (Aboudi, 1991) can be generalized to show

$$\langle \mathbf{Z} \rangle = \mathbf{Z}^o \quad (10)$$

Taking into account the boundary conditions and the effective constitutive equations, we can show

$$\langle \boldsymbol{\Sigma} \rangle = \mathbf{L} \mathbf{Z}^o \quad (11)$$

where \mathbf{L} is the electro-magneto-elastic effective moduli.

We have already noted that $\langle \mathbf{Z} \rangle = \mathbf{Z}^o$. The volume-weighted average of \mathbf{Z} over each phase is expressed as

$$\mathbf{Z}^o = c_m \langle \mathbf{Z}_m \rangle + \sum_{i=1}^{N-1} c_i \langle \mathbf{Z}_i \rangle \quad (12)$$

where the subscript m denotes the matrix and i is used for numbering the dispersed phases. Applying an analogous result for $\langle \boldsymbol{\Sigma} \rangle$, and using the constitutive equations for each phase and the composite yields

$$\mathbf{L} \mathbf{Z}^o = \mathbf{L}_m \mathbf{Z}^o + \sum_{i=1}^{N-1} c_i (\mathbf{L}_i - \mathbf{L}_m) \langle \mathbf{Z}_i \rangle \quad (13)$$

Finally, by simple manipulations, the general expression for the effective properties of perfectly bonded N-phase composites yields

$$\mathbf{L} = \mathbf{L}_m + \sum_{i=1}^{N-1} c_i (\mathbf{L}_i - \mathbf{L}_m) \mathbf{A}_i \quad (14)$$

where \mathbf{A}_i is the concentration factor that relates the average strain and potential gradients in phase i to that in the composite, namely,

$$\langle \mathbf{Z}_i \rangle = \mathbf{A}_i \mathbf{Z}^o \quad (15)$$

The estimation of \mathbf{A}_i is the key to predicting the effective electro-magneto-elastic moduli \mathbf{L} . From the rigorous framework, it is clear that the estimate of the effective properties depends on the estimate of concentration factor \mathbf{A}_i , either directly or indirectly.

B. Mori-Tanaka Method for Three-phase Electro-magneto-elastic Composite

The Mori-Takaka theory is one of the micromechanical approaches to estimating the concentration factor \mathbf{A}_i . The basic assumption of the Mori-Tanaka scheme is that \mathbf{A}_i is given by the solution for a single particle embedded in an infinite matrix subjected to an applied electro-magneto-elastic field equal to the as-yet-unknown average field in the matrix. This assumption is easily expressed as

$$\langle \mathbf{Z}_i \rangle = \mathbf{A}_i^{dil} \langle \mathbf{Z}_m \rangle \quad (16)$$

where \mathbf{A}_i^{dil} is the dilute concentration tensor that can be obtained from electro-magneto-elastic Eshelby tensors \mathbf{S}_i , which are composed of one 4th rank tensor, four 3rd rank tensors, and four 2nd rank tensors. Explicit expressions of the electro-magneto-elastic Eshelby tensors are given by Li and Dunn (1998) and tabulated in the Appendix C. For ellipsoidal inclusions, they are functions of the shape of the inclusion and the electro-magneto-elastic moduli of the matrix.

From the average strain theorem and the definition of the concentration factor, the dilute concentration factor \mathbf{A}_i^{dil} and Mori-Tanaka concentration factor \mathbf{A}_i^{MT} can be shown as

$$\mathbf{A}_i^{dil} = [\mathbf{I} + \mathbf{S}_i \mathbf{L}_m^{-1} (\mathbf{L}_i - \mathbf{L}_m)]^{-1} \quad (17)$$

$$\mathbf{A}_i^{MT} = \mathbf{A}_i^{MT} (c_m \mathbf{I} + \sum_{i=1}^{N-1} c_i \mathbf{A}_i^{dil})^{-1} \quad (18)$$

To apply this to three-phase composites, it is necessary to find \mathbf{A}_i^{dil} and \mathbf{A}_i^{MT} for each inclusion. Because the Eshelby tensor \mathbf{S}_i is a function of the matrix material properties and the shape of inclusions, \mathbf{S}_i is the same for piezomagnetic and piezoelectric phases in the elastic matrix based composite [17].

Finally, the effective moduli can be written in the form

$$\mathbf{L} = \mathbf{L}_m + c_1 (\mathbf{L}_1 - \mathbf{L}_m) \mathbf{A}_1^{MT} + c_2 (\mathbf{L}_2 - \mathbf{L}_m) \mathbf{A}_2^{MT} \quad (19)$$

The effective moduli developed by the Mori-Tanaka mean field theory are functions of the phase volume fraction, the shape of the inclusions and the material properties of each phase.

CHAPTER IV

FINITE ELEMENT METHOD

A. Periodic Unit Cell

The finite element analysis program FEMLAB was used to solve the field equations in a periodic unit cell consisting of two types of fibers separated by a matrix. Several types of periodic unit cells are possible for a three-phase fibrous composite. In this paper, we consider the periodic microstructure and the periodic unit cell of Figure 2.

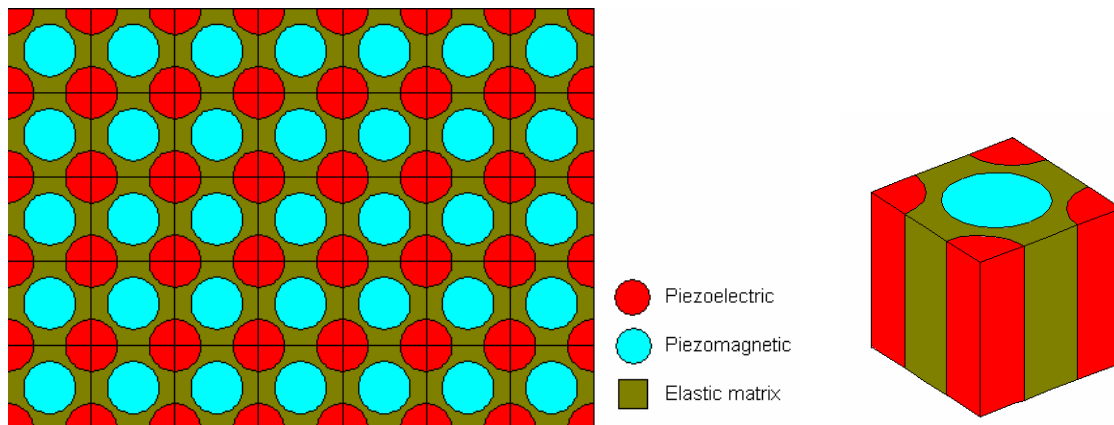


Figure 2. Periodic structure model and Periodic unit cell

B. Periodic Boundary Conditions

When the microstructure model is given, there arises the question of what boundary conditions should be used to determine the effective moduli. We may use the homogeneous stress and strain boundary conditions such that the solutions of the resulting macrofield equations can overestimate or underestimate macroscopic responses

that are obtained by using other effective moduli since these boundary conditions provide upper and lower bounds for all possible effective moduli. However, we may use the periodic boundary conditions that provide the effective moduli, which represent those obtained by using a certain class of boundary conditions [18, 19, 20, 21]. Periodic boundary conditions (Hori and Nematt-Nasser, 1999) are applied to the periodic unit cell, as indicated in Table 1, referenced to Figure 3.

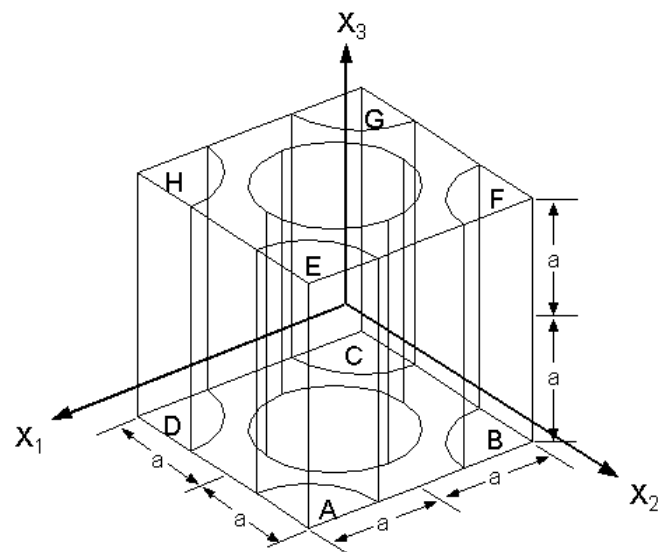


Figure 3. Schematic of the periodic unit cell used for the periodic boundary conditions

Table 1. Boundary condition equations

Between $\square AEHD$ and $\square BFGC$	Between $\square ABFE$ and $\square DCGH$	Between $\square ABCD$ and $\square EFGH$
$u_1(a, x_2, x_3) = u_1(-a, x_2, x_3) + \langle \varepsilon_{11} \rangle 2a$	$u_1(x_1, a, x_3) = u_1(x_1, -a, x_3) + \langle \varepsilon_{21} \rangle 2a$	$u_1(x_1, x_2, a) = u_1(x_1, x_2, -a) + \langle \varepsilon_{31} \rangle 2a$
$u_2(a, x_2, x_3) = u_2(-a, x_2, x_3) + \langle \varepsilon_{12} \rangle 2a$	$u_2(x_1, a, x_3) = u_2(x_1, -a, x_3) + \langle \varepsilon_{22} \rangle 2a$	$u_2(x_1, x_2, a) = u_2(x_1, x_2, -a) + \langle \varepsilon_{32} \rangle 2a$
$u_3(a, x_2, x_3) = u_3(-a, x_2, x_3) + \langle \varepsilon_{13} \rangle 2a$	$u_3(x_1, a, x_3) = u_3(x_1, -a, x_3) + \langle \varepsilon_{23} \rangle 2a$	$u_3(x_1, x_2, a) = u_3(x_1, x_2, -a) + \langle \varepsilon_{33} \rangle 2a$
$\phi(a, x_2, x_3) = \phi(-a, x_2, x_3) - \langle E_1 \rangle 2a$	$\phi(x_1, a, x_3) = \phi(x_1, -a, x_3) - \langle E_2 \rangle 2a$	$\phi(x_1, x_2, a) = \phi(x_1, x_2, -a) - \langle E_3 \rangle 2a$
$\Phi(a, x_2, x_3) = \Phi(-a, x_2, x_3) - \langle H_1 \rangle 2a$	$\Phi(x_1, a, x_3) = \Phi(x_1, -a, x_3) - \langle H_2 \rangle 2a$	$\Phi(x_1, x_2, a) = \Phi(x_1, x_2, -a) - \langle H_3 \rangle 2a$

There can be five periodic boundary equations for each pair of opposite boundaries. Because of symmetry, the following pairs of boundary conditions are equivalent.

$$u_3(x_1, a, x_3) = u_3(x_1, -a, x_3) + \langle \varepsilon_{23} \rangle 2a \Leftrightarrow u_3(a, x_2, x_3) = u_3(-a, x_2, x_3) + \langle \varepsilon_{13} \rangle 2a ;$$

$$u_1(x_1, x_2, a) = u_1(x_1, x_2, -a) + \langle \varepsilon_{31} \rangle 2a \Leftrightarrow u_2(x_1, x_2, a) = u_2(x_1, x_2, -a) + \langle \varepsilon_{32} \rangle 2a ;$$

$$u_2(a, x_2, x_3) = u_2(-a, x_2, x_3) + \langle \varepsilon_{12} \rangle 2a \Leftrightarrow u_1(x_1, a, x_3) = u_1(x_1, -a, x_3) + \langle \varepsilon_{21} \rangle 2a$$

This means that, if one were seeking to independently apply each of the fifteen boundary conditions, three of them would be redundant. Therefore, there are twelve independent boundary value problem cases that would need to be obtained. The bracketed terms are the input values that are the appropriate volume averaged quantity (e.g., the term $\langle \varepsilon_{11} \rangle$, the value supplied, say $\langle \varepsilon_{11} \rangle = 0.001$, would be the average strain).

C. Evaluation of the Effective Constitutive Equations

For example, by specifying an average value for the term $\langle \varepsilon_{11} \rangle$ for one of the independent boundary condition equations and specifying all of the other average values to be zero, one can construct one of the twelve independent boundary value problem cases. Returning to the engineering formulation of the constitutive response for the effective composite, the implementation of this boundary condition would be seen as following:

$$\begin{pmatrix} \langle \sigma_{11} \rangle \\ \langle \sigma_{22} \rangle \\ \langle \sigma_{33} \rangle \\ \langle \sigma_{23} \rangle \\ \langle \sigma_{31} \rangle \\ \langle \sigma_{12} \rangle \\ \langle D_1 \rangle \\ \langle D_2 \rangle \\ \langle D_3 \rangle \\ \langle B_1 \rangle \\ \langle B_2 \rangle \\ \langle B_3 \rangle \end{pmatrix} = \begin{pmatrix} \mathbf{C}^* & \mathbf{e}^{*\text{T}} & \mathbf{q}^{*\text{T}} \\ \mathbf{e}^* & -\boldsymbol{\eta}^* & -\boldsymbol{\lambda}^{*\text{T}} \\ \mathbf{q}^* & -\boldsymbol{\lambda}^* & -\boldsymbol{\mu}^* \end{pmatrix} \begin{pmatrix} \langle \varepsilon_{11} \rangle \\ 0 \\ 0 \\ 0 \\ 0 \\ 0 \\ 0 \\ 0 \\ 0 \\ 0 \\ 0 \\ 0 \end{pmatrix} \quad (20)$$

We may represent the twelve independent applied boundary conditions by collecting them as columns in a matrix in the following way where the associated outputs may also be cast as the columns in an analogous manner.

$$\begin{pmatrix} \langle \sigma_{11} \rangle \\ \langle \sigma_{22} \rangle \\ \langle \sigma_{33} \rangle \\ \langle \sigma_{23} \rangle \\ \langle \sigma_{31} \rangle \\ \langle \sigma_{12} \rangle \\ \langle D_1 \rangle \\ \langle D_2 \rangle \\ \langle D_3 \rangle \\ \langle B_1 \rangle \\ \langle B_2 \rangle \\ \langle B_3 \rangle \end{pmatrix} \begin{pmatrix} \langle \sigma_{11} \rangle \\ \langle \sigma_{22} \rangle \\ \langle \sigma_{33} \rangle \\ \langle \sigma_{23} \rangle \\ \langle \sigma_{31} \rangle \\ \langle \sigma_{12} \rangle \\ \langle D_1 \rangle \\ \langle D_2 \rangle \\ \langle D_3 \rangle \\ \langle B_1 \rangle \\ \langle B_2 \rangle \\ \langle B_3 \rangle \end{pmatrix}^{12 \times 12} = \begin{pmatrix} \mathbf{C}^* & \mathbf{e}^{*T} & \mathbf{q}^{*T} \\ \mathbf{e}^* & -\boldsymbol{\eta}^* & -\boldsymbol{\lambda}^{*T} \\ \mathbf{q}^* & -\boldsymbol{\lambda}^* & -\boldsymbol{\mu}^* \end{pmatrix} \begin{pmatrix} \langle \varepsilon_{11} \rangle & 0 & 0 & 0 & 0 & 0 & 0 & 0 & 0 & 0 & 0 & 0 \\ 0 & \langle \varepsilon_{22} \rangle & 0 & 0 & 0 & 0 & 0 & 0 & 0 & 0 & 0 & 0 \\ 0 & 0 & \langle \varepsilon_{33} \rangle & 0 & 0 & 0 & 0 & 0 & 0 & 0 & 0 & 0 \\ 0 & 0 & 0 & 2\langle \varepsilon_{23} \rangle & 0 & 0 & 0 & 0 & 0 & 0 & 0 & 0 \\ 0 & 0 & 0 & 0 & 2\langle \varepsilon_{31} \rangle & 0 & 0 & 0 & 0 & 0 & 0 & 0 \\ 0 & 0 & 0 & 0 & 0 & 2\langle \varepsilon_{12} \rangle & 0 & 0 & 0 & 0 & 0 & 0 \\ 0 & 0 & 0 & 0 & 0 & 0 & -\langle E_1 \rangle & 0 & 0 & 0 & 0 & 0 \\ 0 & 0 & 0 & 0 & 0 & 0 & 0 & -\langle E_2 \rangle & 0 & 0 & 0 & 0 \\ 0 & 0 & 0 & 0 & 0 & 0 & 0 & 0 & -\langle E_3 \rangle & 0 & 0 & 0 \\ 0 & 0 & 0 & 0 & 0 & 0 & 0 & 0 & 0 & -\langle H_1 \rangle & 0 & 0 \\ 0 & 0 & 0 & 0 & 0 & 0 & 0 & 0 & 0 & 0 & -\langle H_2 \rangle & 0 \\ 0 & 0 & 0 & 0 & 0 & 0 & 0 & 0 & 0 & 0 & 0 & -\langle H_3 \rangle \end{pmatrix} \quad (21)$$

Therefore, we can construct a 12x12 input matrix and a 12x12 output matrix.

These two matrices may be used to solve for the values of the 12x12 effective property matrix.

D. Element and Solver

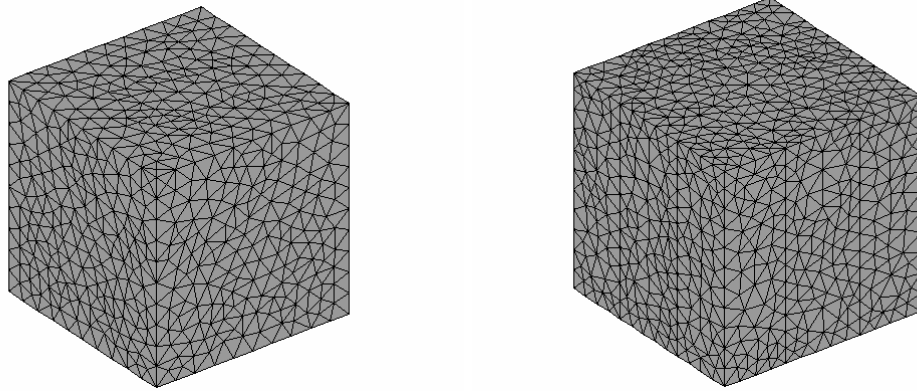


Figure 4. Mesh shape of two-phase composite and three-phase composite

The mesh used in the FEM analysis for two-phase composites and three-phase composites are shown in Figure 4. The number of elements for each model are 16,207

and 21,824, respectively. The tetrahedron linear elements are used for FEA. Analysis is carried out using a linear iterative solver.

CHAPTER V

RESULTS AND DISCUSSION

A. Two-phase Electro-magneto-elastic Composite

Before considering the three-phase composite, we first verified our analytical procedure by comparing the results of the finite element analysis with published results for the Mori-Tanaka method (Li and Dunn (1998)) for a two-phase composite consisting of a piezomagnetic matrix ($CoFe_2O_4$, Table 2) reinforced with piezoelectric fibers ($BaTiO_3$, Table 2). Both phases are transversely isotropic with x_3 the axis of symmetry.

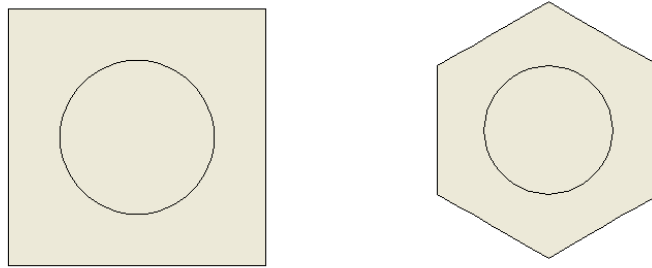


Figure 5. Square unit cell and hexagonal unit cell

For unidirectionally fiber reinforced composites, various types of periodic unit cells are possible. However, frequently employed idealized fibrous-matrix unit cells are square unit cell and hexagonal unit cell as seen in Figure 5. An important characteristic of these composites is their transverse isotropy. A square periodic unit cell is relatively more frequently employed than a hexagonal unit cell in the literature. However, a square periodic unit cell lacks transverse isotropy that most unidirectional composites,

consisting of a matrix reinforced with randomly distributed fibers, possess owing to the random distribution of fibers in the matrix. If the transverse isotropy is not the characteristic to be preserved through the idealization, then advantage can be taken of its simplicity by comparing with other types of unit cell. The superiority of the hexagonal unit cell to the square unit cell is that it preserves the transverse isotropic characteristic while the effective properties obtained from the square unit cell show significant transverse anisotropy. However, the transverse isotropy achieved through a hexagonal unit cell is at a price (i.e. the unit cell from it is substantially more sophisticated than that from a square unit cell) [22, 23, 24]. The basic assumption of the Mori-Tanaka theory used by Li and Dunn (1998) to determine the effective properties of a two-phase electro-magneto-elastic composite is that the dispersed fibers are perfectly aligned. This means that the effective moduli determined by the Mori-Tanaka theory preserves the transverse isotropy [25, 26].

Thus, the proper unit cell for the FEM to compare with the Mori-Tanaka method by Li and Dunn (1998) may be the hexagonal unit cell. However, we consider the square unit cell for a two-phase electro-magneto-elastic composite with the benefit of simplicity and also because we take into account the square unit cell for a three-phase electro-magneto-elastic composite.

The stiffness tensor of materials that show transverse isotropy behavior has six different components (Equation 2a). However, there exist only five independent components by the relation between the components as following

$$\frac{C_{11} - C_{12}}{2} - C_{66} = 0 \quad (22)$$

Figures 6 through 8 show the distribution of the stiffness tensor for the rotational variation and the average of varying values. To verify the transverse isotropy, the relation between the components and the normalized average of varying values are plotted in Figure 9. Equation 22 is satisfied for the averaged components as seen in Figure 9. Thus, the rotationally averaged stiffness tensor shows the transverse isotropy.

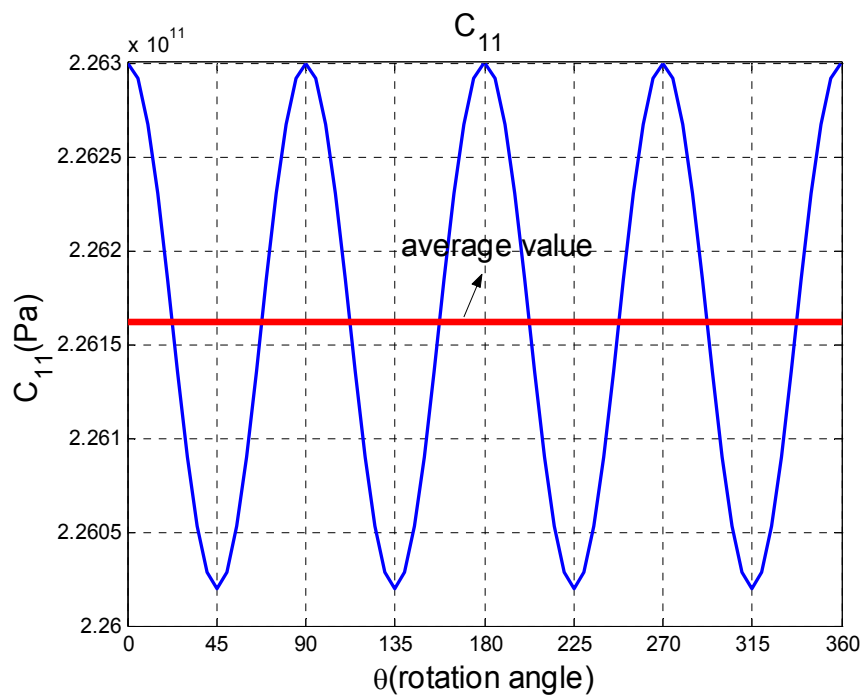


Figure 6. C_{11} distribution for rotational variation for a two-phase composite

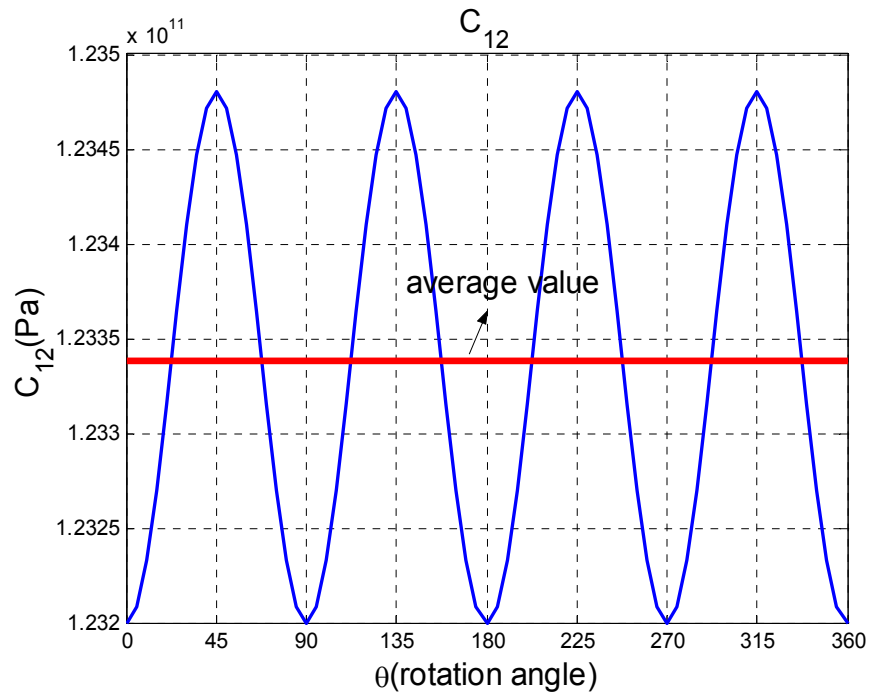


Figure 7. C_{12} distribution for rotational variation for a two-phase composite

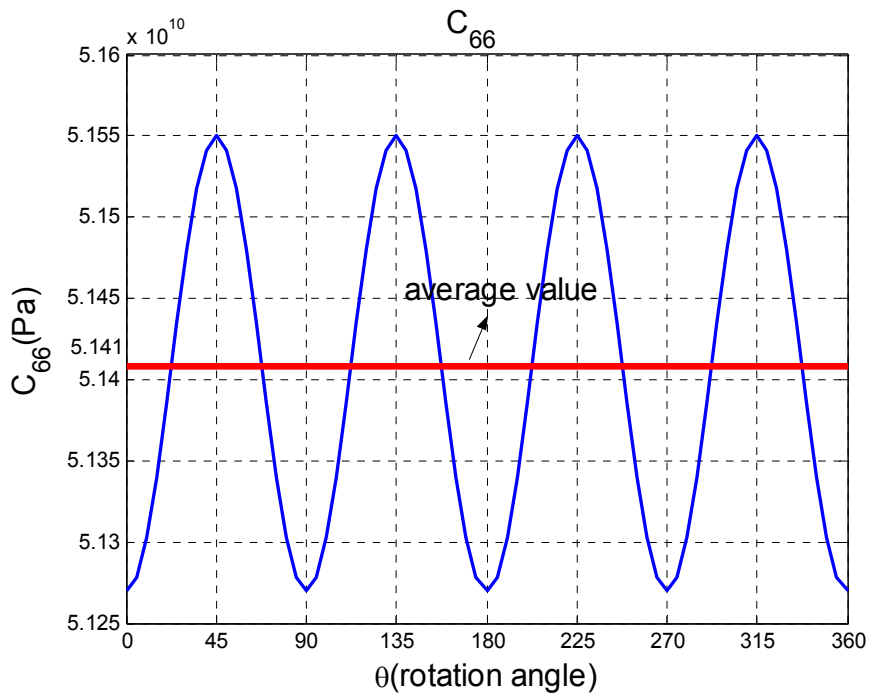


Figure 8. C_{66} distribution for rotational variation for a two-phase composite

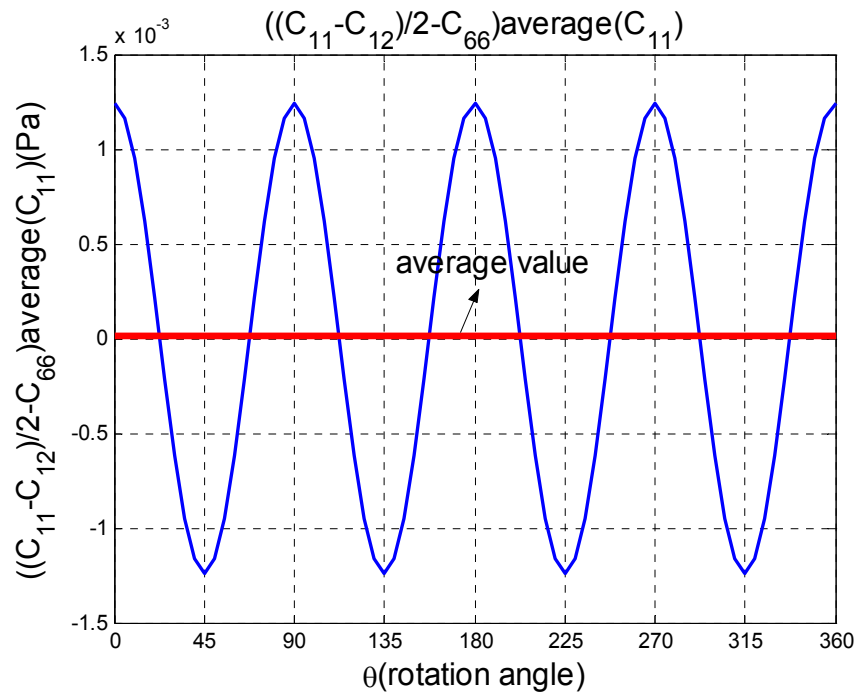


Figure 9. Difference distribution for rotational variation for a two-phase composite

The effective moduli of the fibrous two-phase composite were evaluated for two fiber volume fractions, $v_f=0.4$ and $v_f=0.6$.

The averaged results for the rotational variation are compared with the predictions of Li and Dunn (1998) in Figures 10 through 16, in which the effective moduli determined by the finite element analysis are represented by dots.

The finite element results are in excellent agreement with the Mori-Tanaka results of Li and Dunn (1998) and satisfy Benveniste's (1995) exact connections between the effective moduli.

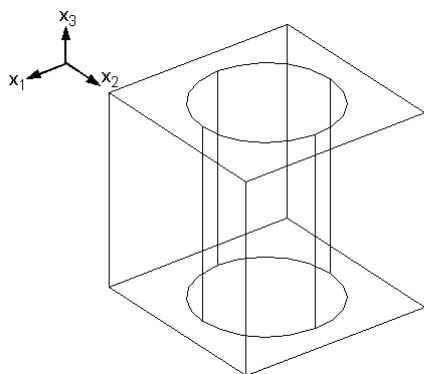


Figure 10. The unit cell of a fibrous two-phase composite.

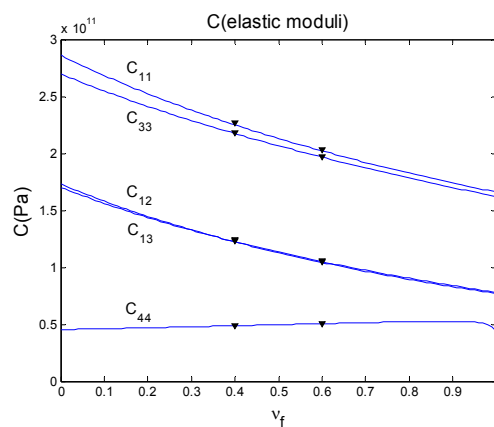


Figure 11. Effective elastic moduli of a fibrous two-phase composite vs v_f

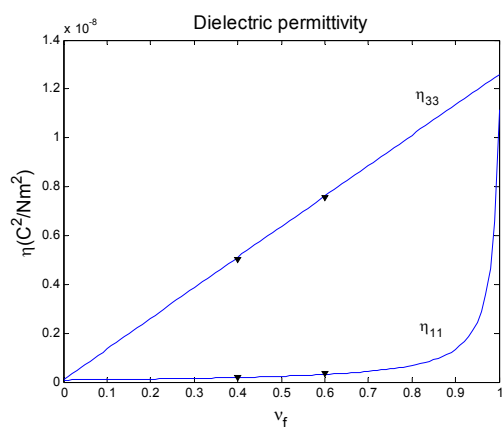


Figure 12. Effective dielectric moduli of a fibrous two-phase composite vs v_f

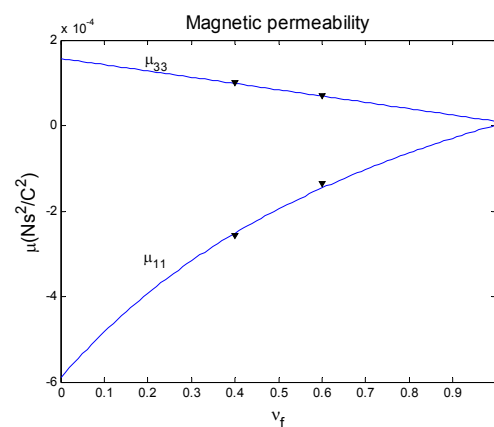


Figure 13. Effective magnetic moduli of a fibrous two-phase composite vs v_f

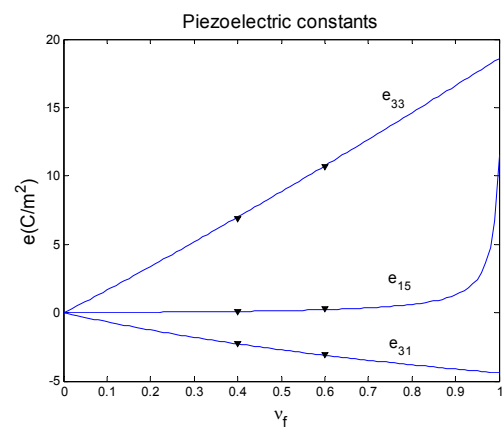


Figure 14. Effective piezoelectric moduli of a fibrous two-phase composite vs v_f

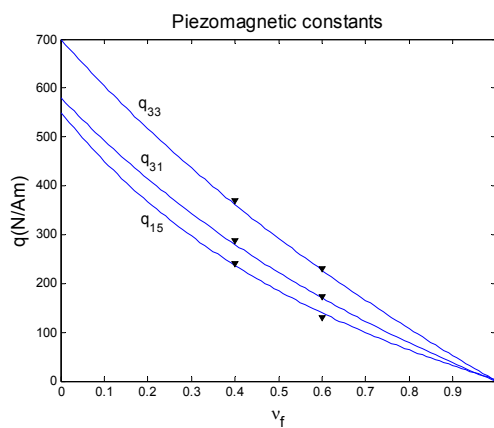


Figure 15. Effective piezomagnetic moduli of a fibrous two-phase composite vs v_f

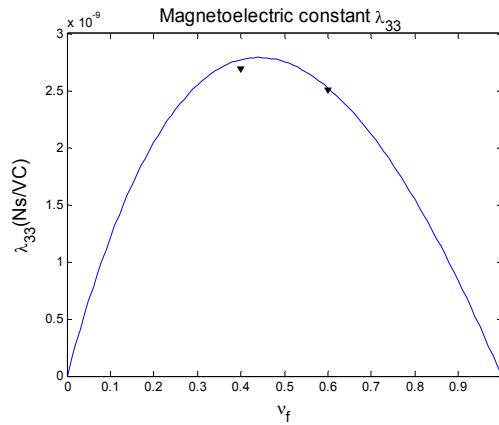


Figure 16. Effective magnetolectric constant λ_{33} of a fibrous two-phase composite vs v_f

Material properties of the piezoelectric phase and the piezomagnetic phase are shown in Table 2.

Table 2. Material properties of $BaTiO_3$ and $CoFe_2O_4$

	$BaTiO_3$ (piezoelectric phase)	$CoFe_2O_4$ (piezomagnetic phase)
C_{11} (Pa)	16.6×10^{10}	28.6×10^{10}
C_{12} (Pa)	7.7×10^{10}	17.3×10^{10}
C_{13} (Pa)	7.8×10^{10}	17.05×10^{10}
C_{33} (Pa)	16.2×10^{10}	26.95×10^{10}
C_{44} (Pa)	4.3×10^{10}	4.53×10^{10}
η_{11} (C^2 / Nm^2)	112×10^{-10}	0.8×10^{-10}
η_{33} (C^2 / Nm^2)	126×10^{-10}	0.93×10^{-10}
μ_{11} (Ns^2 / C^2)	5×10^{-6}	-590×10^{-6}
μ_{33} (Ns^2 / C^2)	10×10^{-6}	157×10^{-6}
e_{31} (C / m^2)	-4.4	0
e_{33} (C / m^2)	18.6	0
e_{15} (C / m^2)	11.6	0
q_{31} (N / Am)	0	5.803×10^2
q_{33} (N / Am)	0	6.997×10^2
q_{15} (N / Am)	0	5.5×10^2

B. Three-phase Electro-magneto-elastic Composite

The phase volume fractions are 0.3, 0.3 and 0.4 for the piezomagnetic fiber ($CoFe_2O_4$, Table 2), the piezoelectric fiber ($BaTiO_3$, Table 2), and the matrix, respectively. The isotropic linear elastic matrix is assumed to be epoxy, so that $C_{11} = 5.53 \times 10^9$ (Pa), $C_{12} = 2.97 \times 10^9$ (Pa), $\eta = 1.0 \times 10^{-10}$ (C^2 / Nm^2), and $\mu = 1.0 \times 10^{-6}$ (Ns^2 / C^2). Figures 17 through 21 show the distributions of electric potential, electric field E_1 , shear strain ε_{31} , magnetic field H_1 , and magnetic potential, respectively, when one of the twelve independent boundary conditions, the electric field $\langle E_1 \rangle$, is applied. $\langle E_1 \rangle$ induces the E_1 distribution of Figure 18, which, in turn, results in the shear strain distribution of Figure 19. The strain in the piezomagnetic fiber results in the magnetic field distribution of Figure 20. Thus, the three-phase composite exhibits the magnetoelectric effect by coupling the piezomagnetic and piezoelectric fibers through the strain in the elastic matrix.

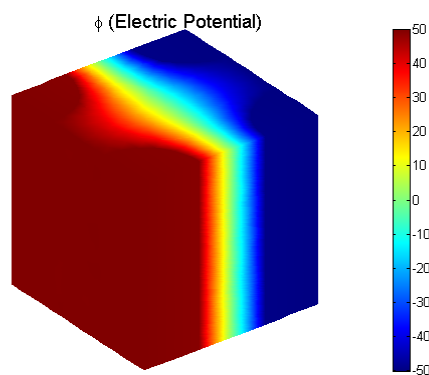


Figure 17. Electric potential distribution of a fibrous three-phase electro-magneto-elastic composite when $\langle E_1 \rangle$ is applied

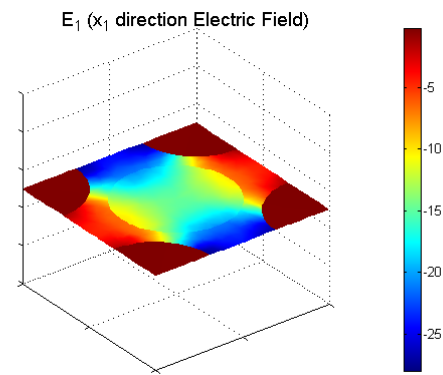


Figure 18. Electric field E_1 distribution of a fibrous three-phase electro-magneto-elastic composite when $\langle E_1 \rangle$ is applied

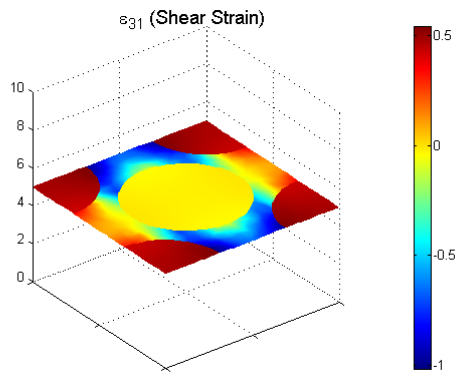


Figure 19. Shear strain ε_{31} distribution of a fibrous three-phase electro-magneto-elastic composite when $\langle E_1 \rangle$ is applied

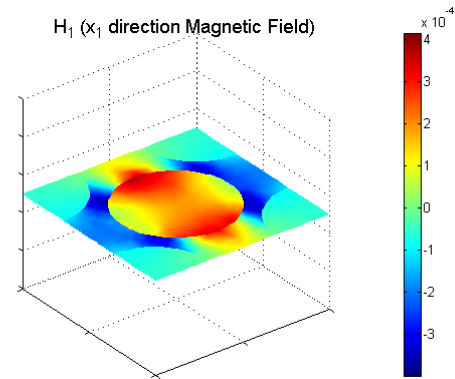


Figure 20. Magnetic field H_1 distribution of a fibrous three-phase electro-magneto-elastic composite when $\langle E_1 \rangle$ is applied

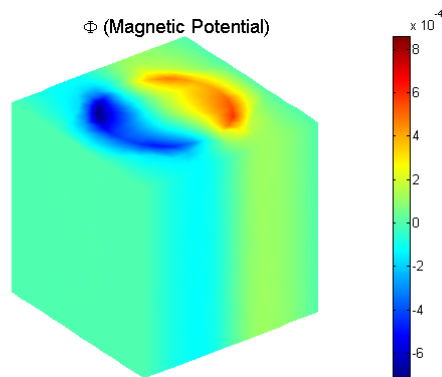


Figure 21. Magnetic potential distribution of a fibrous three-phase electro-magneto-elastic composite when $\langle E_1 \rangle$ is applied

Applying the remaining eleven independent boundary conditions and solving for the effective properties of the composite as previously discussed, we obtain the 12x12 effective moduli (refer back to Equation 23) of the three-phase composite from the finite element method results. Note that the effective magnetoelectric moduli of the three-phase composite are about twenty times less than those of the two-phase composite (Figure 16). This is due to the fact that the stiffness of the elastic matrix used in the

three-phase composite is two orders of magnitude less than those of the piezomagnetic and piezoelectric phases. Thus, although the matrix of the three-phase composite is strained, it lacks sufficient stiffness to transfer these strains to the piezomagnetic fiber.

$$\mathbf{L} = \begin{pmatrix} \mathbf{C}^*(Pa) & \mathbf{e}^{*\top}(C/m^2) & \mathbf{q}^{*\top}(N/Am) \\ \mathbf{e}^*(C/m^2) & -\boldsymbol{\eta}^*(C^2/Nm^2) & -\boldsymbol{\lambda}^{*\top}(Ns/VC) \\ \mathbf{q}^*(N/Am) & -\boldsymbol{\lambda}^*(Ns/VC) & -\boldsymbol{\mu}^*(Ns^2/C^2) \end{pmatrix} =$$

1.596E+10	8.836E+09	8.616E+09	0	0	0	0	0	-1.510E-01	0	0	1.061E+01
8.836E+09	1.596E+10	8.616E+09	0	0	0	0	0	-1.511E-01	0	0	1.060E+01
8.616E+09	8.616E+09	8.333E+10	0	0	0	0	0	6.283E+00	0	0	8.749E+01
0	0	0	5.072E+09	0	0	0	9.842E-03	0	0	-1.790E-01	0
0	0	0	0	5.072E+09	0	9.815E-03	0	0	-1.795E-01	0	0
0	0	0	0	0	6.917E+09	0	0	0	0	0	0
0	0	0	0	9.815E-03	0	-1.716E-10	0	0	-2.689E-13	0	0
0	0	0	9.842E-03	0	0	0	-1.716E-10	0	0	-2.700E-13	0
-1.510E-01	-1.511E-01	6.283E+00	0	0	0	0	0	-3.869E-09	0	0	-1.169E-10
0	0	0	0	-1.795E-01	0	-2.689E-13	0	0	-3.137E-06	0	0
0	0	0	-1.790E-01	0	0	0	-2.702E-13	0	0	-3.136E-06	0
1.061E+01	1.060E+01	8.749E+01	0	0	0	0	0	-1.169E-10	0	0	-5.061E-05

(23)

Note that all the zero terms of the effective matrix generated by the FEM are not exactly zero. The terms which are over three orders less than the other terms are ignored to be zero regarding as the numerical error.

Although the piezoelectric phase and piezomagnetic phase are transversely isotropic materials and the matrix is isotropic, the effective properties of the composite with the square periodic structure are not transversely isotropic. Figures 22 through 24 show the distributions of the stiffness tensor for the rotational variation and the average of varying values. The relation between the components to verify the transverse isotropy (Equation 22) and the normalized average value are plotted in Figure 25. The rotationally averaged stiffness tensor proves the transverse isotropy property.

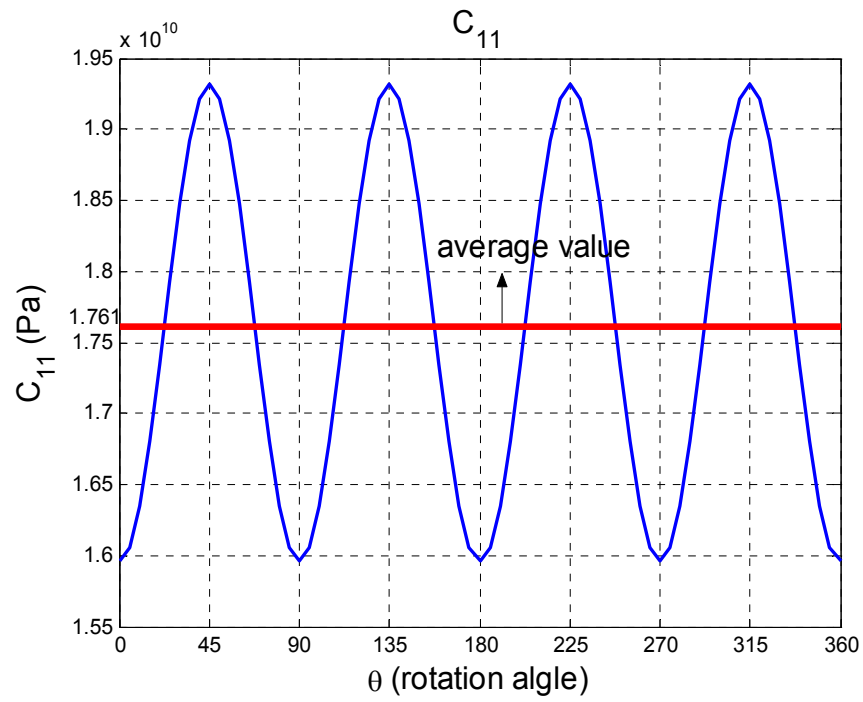


Figure 22. C_{11} distribution for rotational variation for a three-phase composite

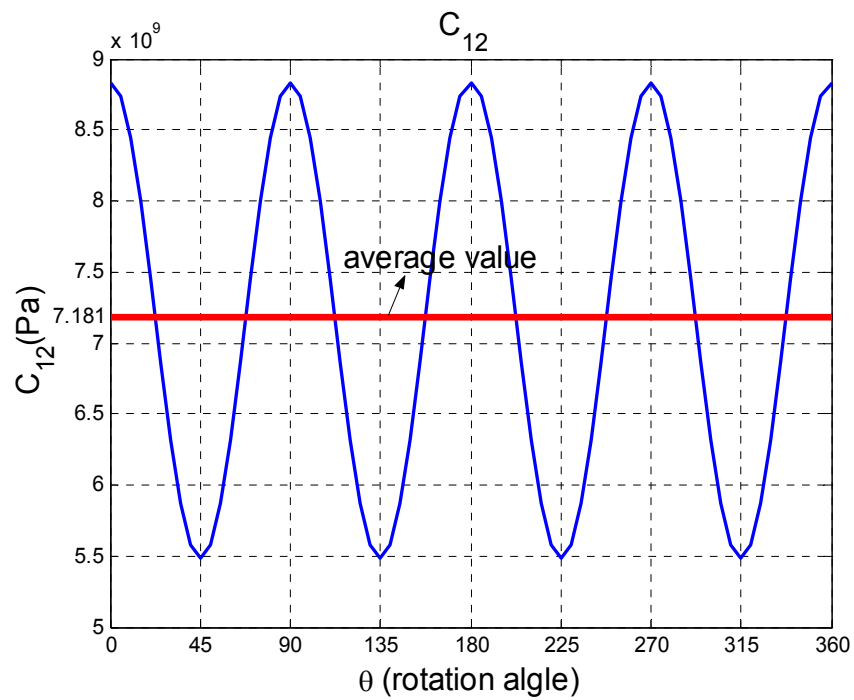


Figure 23. C_{12} distribution for rotational variation for a three-phase composite

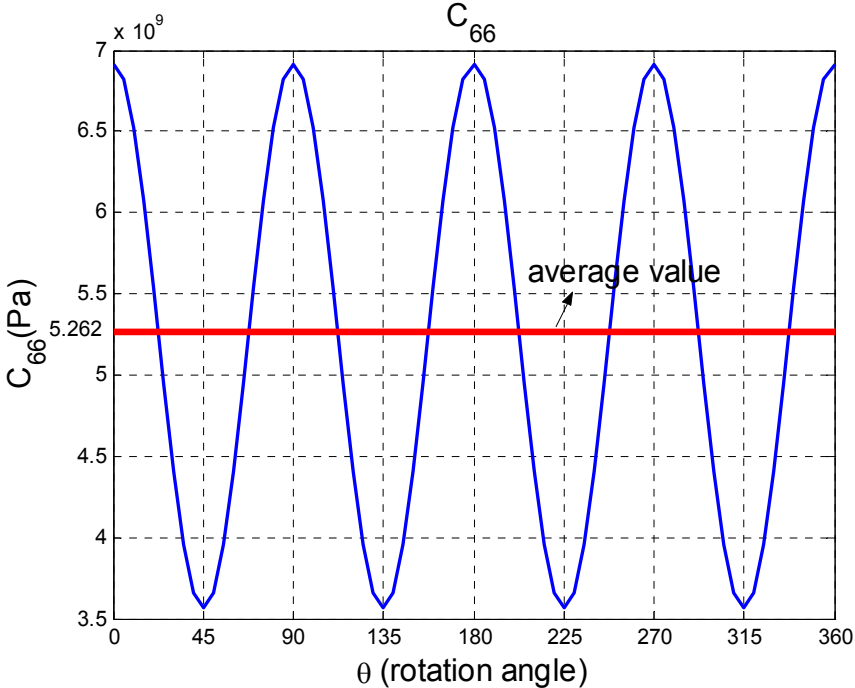


Figure 24. C_{66} distribution for rotational variation for a three-phase composite

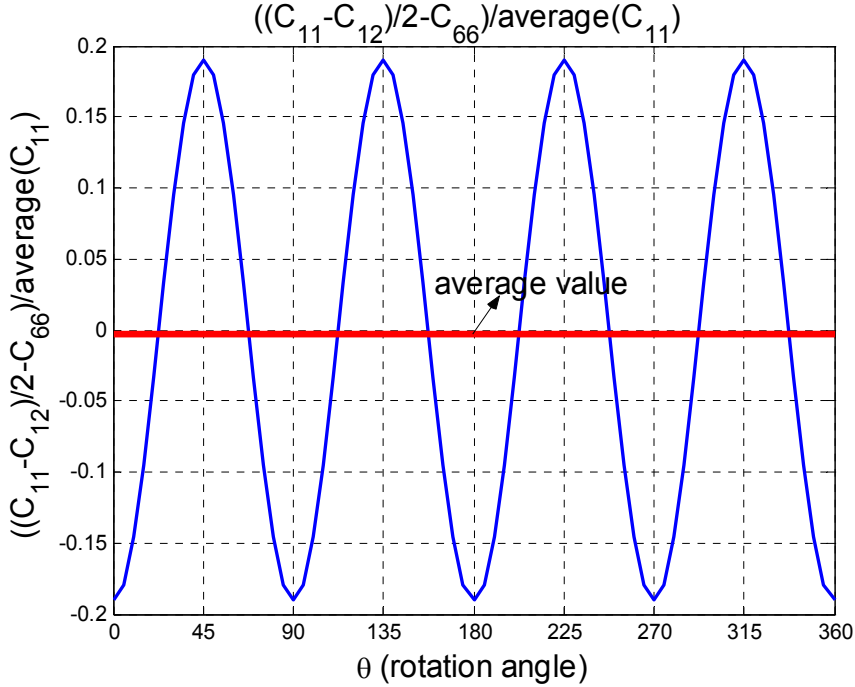


Figure 25. Difference distribution for rotational variation for a three-phase composite

The rotationally averaged effective matrix and the effective matrix determined by the Mori-Tanaka method are shown in Equation 24 and Equation 25, respectively.

Effective moduli determined by the FEM and averaged for the rotational variation

1.761E+10	7.181E+09	8.616E+09	0	0	0	0	0	-1.510E-01	0	0	1.061E+01
7.181E+09	1.761E+10	8.616E+09	0	0	0	0	0	-1.511E-01	0	0	1.060E+01
8.616E+09	8.616E+09	8.333E+10	0	0	0	0	0	6.283E+00	0	0	8.749E+01
0	0	0	5.072E+09	0	0	0	9.828E-03	0	0	-1.792E-01	0
0	0	0	0	5.072E+09	0	0	9.828E-03	0	0	-1.792E-01	0
0	0	0	0	0	5.262E+09	0	0	0	0	0	0
0	0	0	0	9.828E-03	0	0	-1.716E-10	0	0	-2.694E-13	0
0	0	0	9.828E-03	0	0	0	0	-1.716E-10	0	0	-2.694E-13
-1.510E-01	-1.511E-01	6.283E+00	0	0	0	0	0	0	-3.869E-09	0	-1.169E-10
0	0	0	0	-1.792E-01	0	0	-2.694E-13	0	0	-3.136E-06	0
0	0	0	-1.792E-01	0	0	0	0	-2.694E-13	0	0	-3.136E-06
1.061E+01	1.060E+01	8.749E+01	0	0	0	0	0	0	-1.169E-10	0	-5.061E-05

(24)

Effective moduli determined by the Mori-Tanaka method

1.596E+10	7.786E+09	8.254E+09	0	0	0	0	0	-1.414E-01	0	0	9.921E+00
7.786E+09	1.596E+10	8.254E+09	0	0	0	0	0	-1.414E-01	0	0	9.921E+00
8.254E+09	8.254E+09	8.355E+10	0	0	0	0	0	6.330E+00	0	0	8.752E+01
0	0	0	4.658E+09	0	0	0	8.821E-03	0	0	-1.447E-01	0
0	0	0	0	4.658E+09	0	0	8.821E-03	0	0	-1.447E-01	0
0	0	0	0	0	4.088E+09	0	0	0	0	0	0
0	0	0	0	8.821E-03	0	0	-1.712E-10	0	0	-2.150E-13	0
0	0	0	8.821E-03	0	0	0	0	-1.712E-10	0	0	-2.150E-13
-1.414E-01	-1.414E-01	6.330E+00	0	0	0	0	0	0	-3.894E-09	0	-1.067E-10
0	0	0	0	-1.447E-01	0	0	-2.150E-13	0	0	-3.008E-06	0
0	0	0	-1.447E-01	0	0	0	0	-2.150E-13	0	0	-3.008E-06
9.921E+00	9.921E+00	8.752E+01	0	0	0	0	0	0	-1.067E-10	0	-5.093E-05

(25)

C. Parametric Studies

The effective electric, magnetic, mechanical, and coupled-field properties are functions of phase volume fractions, the poling directions of piezoelectric phase and

piezomagnetic phase, the fiber (or particle) shapes, the fiber arrangements in the unit cell and the fiber material properties. Finite element analysis is used to determine the effective properties with special emphasis on the phase volume fraction and the poling directions of the piezoelectric and piezomagnetic fibers. The results were compared with those of Mori-Tanaka method.

1. Effects of volume fractions

a. Fixed elastic matrix volume fraction

Considering first the effect of varying the relative volume fraction of the piezo materials, the matrix volume fraction is fixed at 0.4. The volume fraction of the fibrous piezomagnetic phase is denoted by ν_f . In this case, the effective elastic, electric, magnetic and electromagnetic coupling moduli of three-phase composite are generated for $0 \leq \nu_f \leq 0.6$. The FEM results are compared with the Mori-Tanaka results in Figures 26 through 37, in which the effective moduli determined by the finite element analysis are presented by triangles.

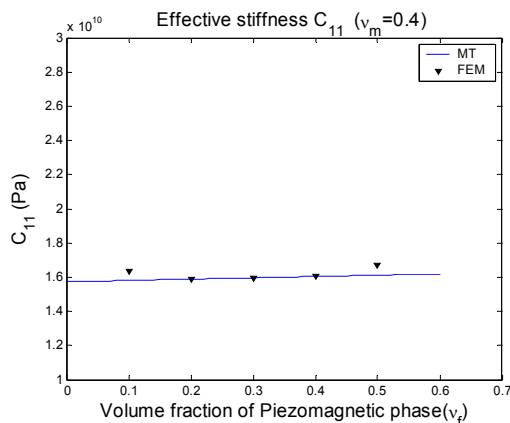


Figure 26. Effective stiffness C_{11} vs V_f

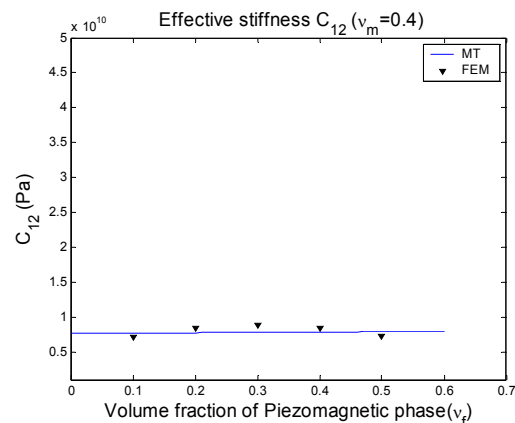


Figure 27. Effective stiffness C_{12} vs V_f

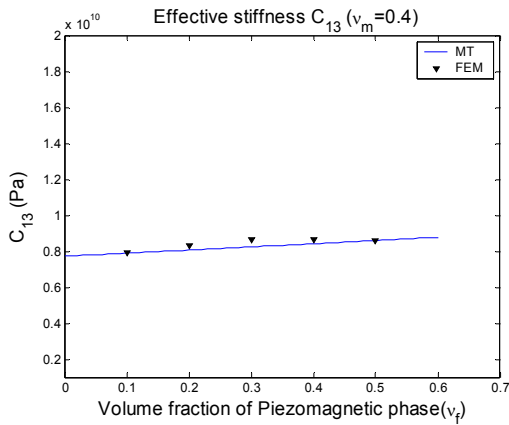


Figure 28. Effective stiffness C_{13} vs V_f

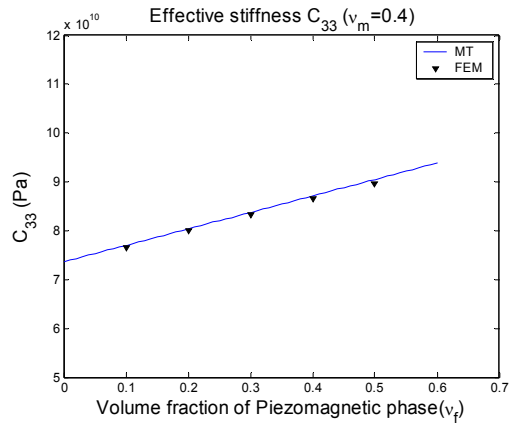


Figure 29. Effective stiffness C_{33} vs V_f

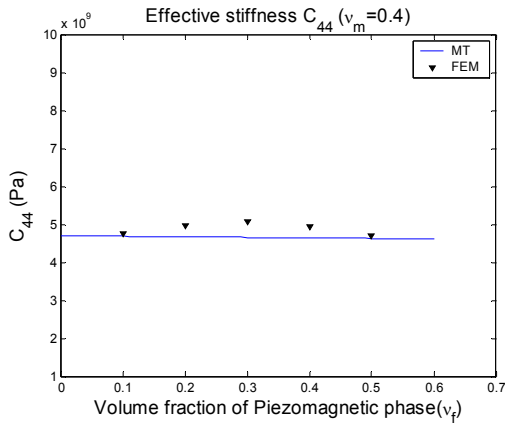


Figure 30. Effective stiffness C_{44} vs V_f

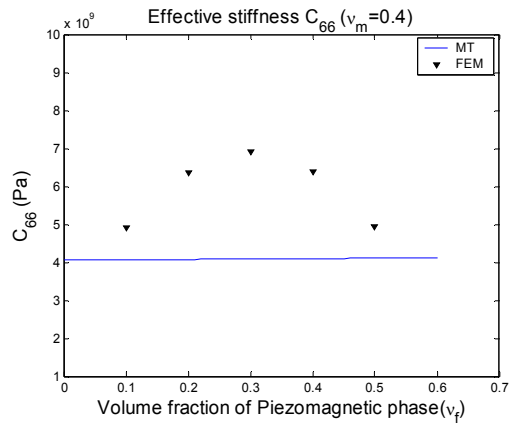


Figure 31. Effective stiffness C_{66} vs V_f

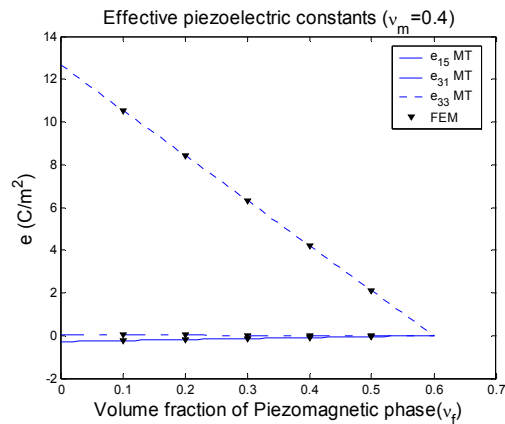


Figure 32. Effective piezoelectric constants vs V_f

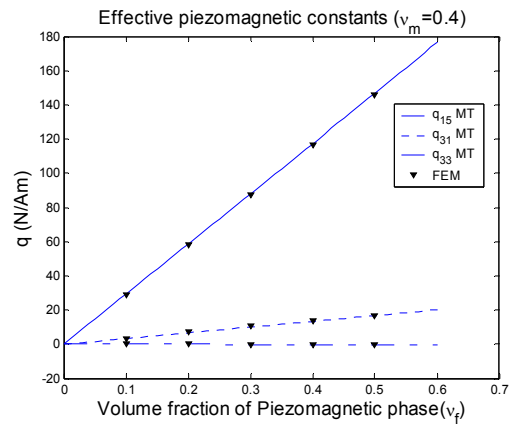
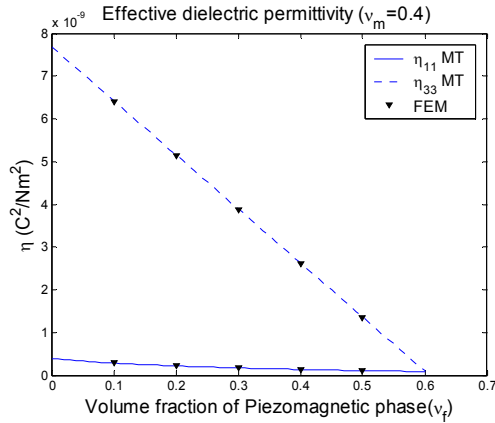
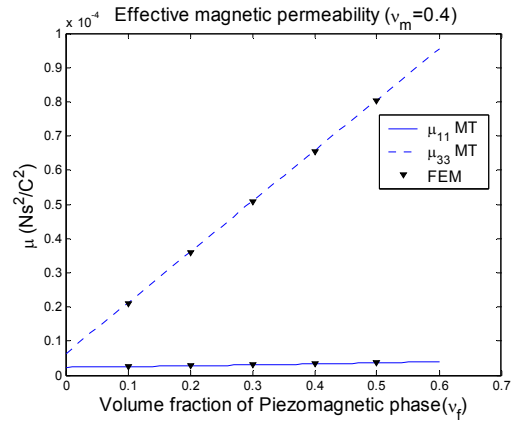
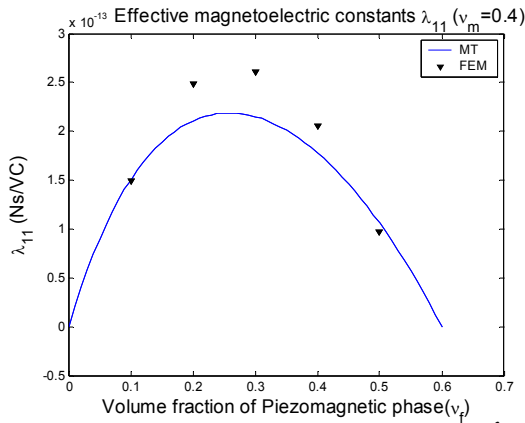
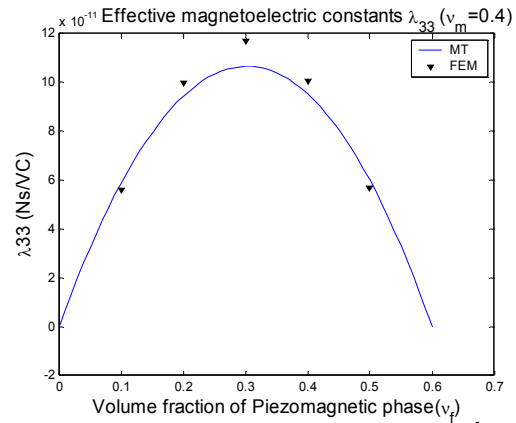


Figure 33. Effective piezomagnetic constants vs V_f

Figure 34. Effective dielectric permittivity vs v_f Figure 35. Effective magnetic permeability vs v_f Figure 36. Effective magnetolectric constant λ_{11} vs v_f Figure 37. Effective magnetolectric constant λ_{33} vs v_f

In some cases, the FEM results and Mori-Tanaka results coincide, while in other cases slight deviations are observed. Because the effective moduli predicted by the Mori-Tanaka method are functions of the phase volume fractions, the fiber shapes and the phase material properties, the Mori-Tanaka theory can not recognize particular arrangement of the fibers. The effective stiffness constants in Figure 26 through 31 generated by the Mori-Tanaka method show linear distributions by the volume change.

On the other hand, the effective stiffness determined by the FEM, which recognize the specific arrangement of the fibers, show nonlinear behavior.

Figures 36 and 37 indicate that the magnetolectric coupling constants are maximum when the piezoelectric volume fraction and the piezomagnetic volume fraction are approximately in a 1:1 ratio.

b. Fixed piezoelectric and piezomagnetic volume ratio

Numerical calculations for four different elastic volume fraction cases are obtained for a fixed volume fraction ratio of the piezoelectric phase to the piezomagnetic phase. The ratio of 1:1 is chosen at which the magnetolectric coupling constants show their maximum value. The volume fraction of the elastic matrix is denoted by ν_m . In this case, the effective elastic, electric, magnetic and electromagnetic coupling moduli of three-phase composite are generated for $0.3 \leq \nu_m \leq 0.6$. The FEM results are compared with the Mori-Tanaka results in Figures 38 through 49, in which the effective moduli determined by the finite element analysis are presented by triangles.

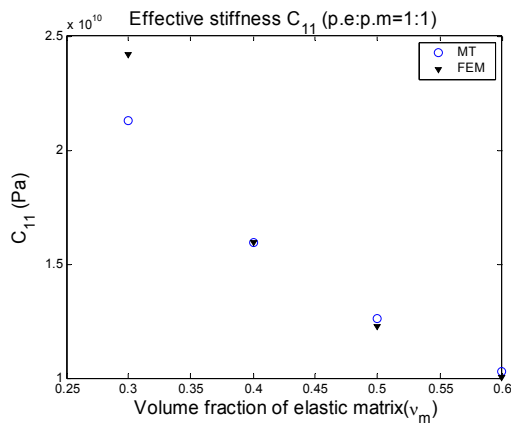


Figure 38. Effective stiffness C_{11} vs ν_m

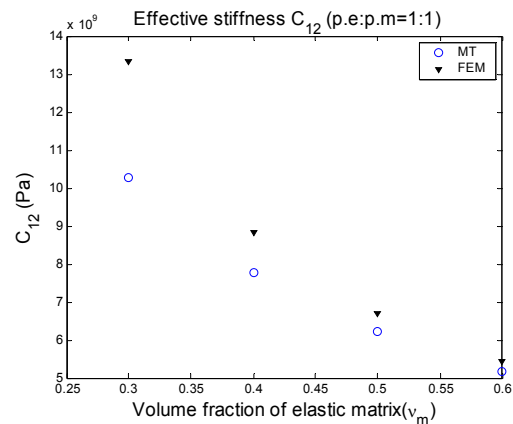


Figure 39. Effective stiffness C_{12} vs ν_m

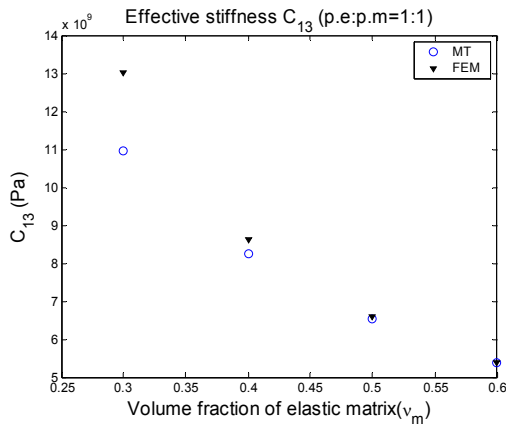


Figure 40. Effective stiffness C_{13} vs V_m

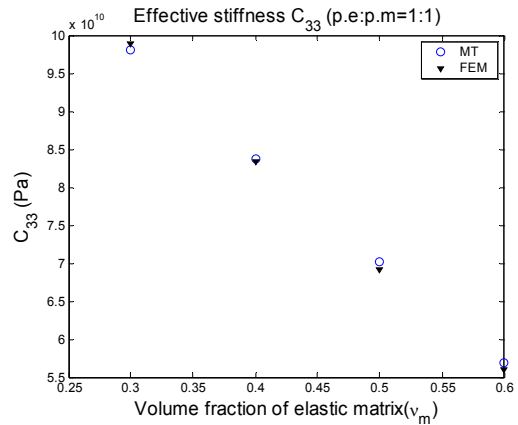


Figure 41. Effective stiffness C_{33} vs V_m

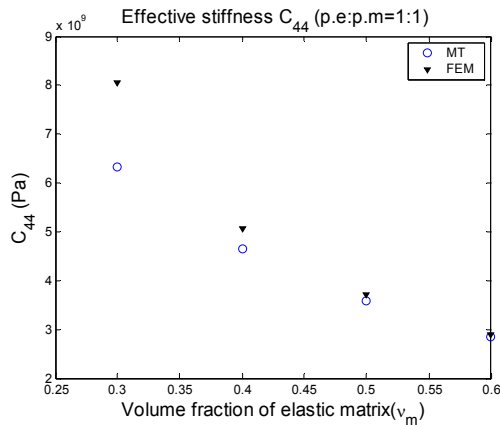


Figure 42. Effective stiffness C_{44} vs V_m

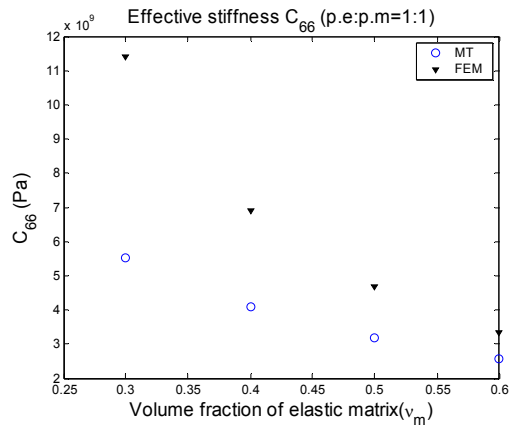


Figure 43. Effective stiffness C_{66} vs V_m

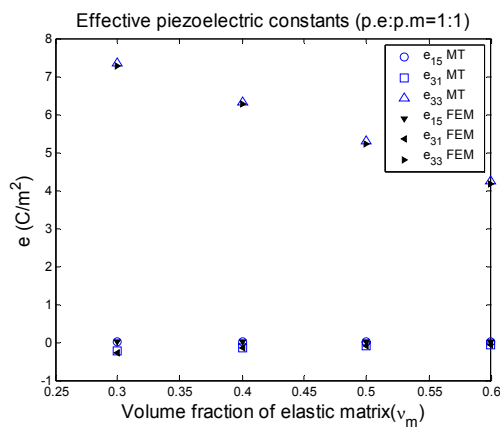


Figure 44. Effective piezoelectric constants vs V_m

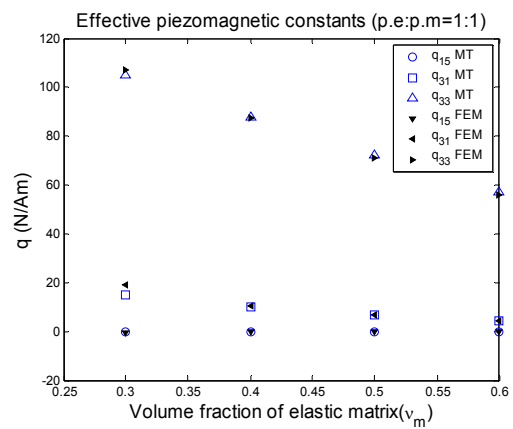
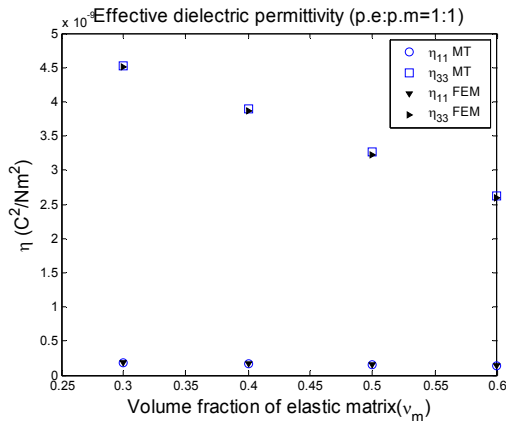
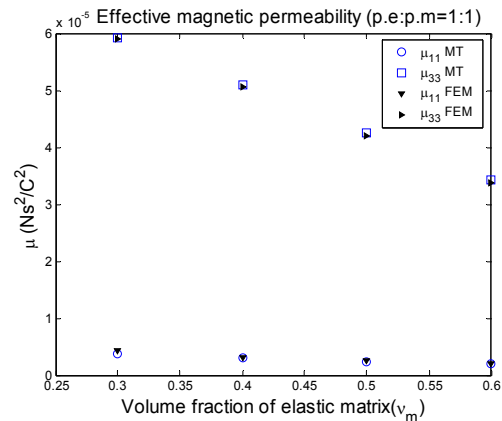
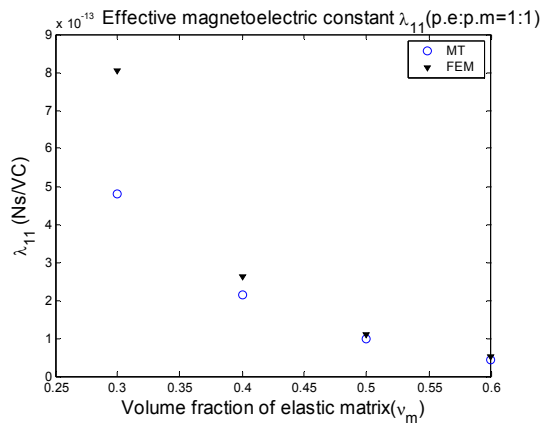
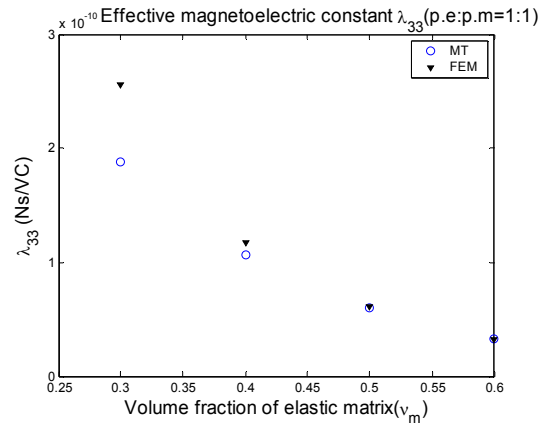


Figure 45. Effective piezomagnetic constants vs V_m

Figure 46. Effective dielectric permittivity vs v_m Figure 47. Effective magnetic permeability vs v_m Figure 48. Effective magnetolectric constant λ_{11} vs v_m Figure 49. Effective magnetolectric constant λ_{33} vs v_m

The effective magnetolectric constants of the three-phase composite decrease as the matrix volume fraction increase.

Note that the differences between the two methods decrease as the volume fraction of the elastic matrix increases. The FEM results and Mori-Tanaka results coincide when the matrix volume fraction is 0.6.

2. Effects of poling direction

In section B, the piezoelectric and piezomagnetic phases are poled in the x_3 direction. In this section, the poling directions will be expressed in a vector component form (x_1, x_2, x_3) . The FEM results are compared with the Mori-Tanaka results for four different poling cases (Table 3). The phase volume fractions are 0.3, 0.3 and 0.4 for the piezoelectric fiber, the piezomagnetic fiber, and the matrix, respectively. Recall that the fibers are aligned in the x_3 direction (Figure 3). Equations 26 through 33 show the effective moduli determined by the Mori-Tanaka method and the FEM for each case.

Table 3. Poling directions of each case

	Piezoelectric phase poling direction	Piezomagnetic phase poling direction
Case (1)	(0,0,1)	(0,0,1)
Case (2)	(1,0,0)	(0,0,1)
Case (3)	(0,0,1)	(1,0,0)
Case (4)	(0,1,0)	(0,1,0)

Case (1)

Effective moduli determined by the Mori-Tanaka method

1.596E+10	7.786E+09	8.254E+09	0	0	0	0	0	-1.414E-01	0	0	9.921E+00
7.786E+09	1.596E+10	8.254E+09	0	0	0	0	0	-1.414E-01	0	0	9.921E+00
8.254E+09	8.254E+09	8.355E+10	0	0	0	0	0	6.330E+00	0	0	8.752E+01
0	0	0	4.658E+09	0	0	0	0	8.821E-03	0	0	-1.447E-01
0	0	0	0	4.658E+09	0	0	8.821E-03	0	0	-1.447E-01	0
0	0	0	0	0	4.088E+09	0	0	0	0	0	0
0	0	0	0	8.821E-03	0	0	-1.712E-10	0	0	-2.150E-13	0
0	0	0	8.821E-03	0	0	0	0	-1.712E-10	0	0	-2.150E-13
-1.414E-01	-1.414E-01	6.330E+00	0	0	0	0	0	0	-3.894E-09	0	-1.067E-10
0	0	0	0	-1.447E-01	0	0	-2.150E-13	0	0	-3.008E-06	0
0	0	0	-1.447E-01	0	0	0	0	-2.150E-13	0	0	-3.008E-06
9.921E+00	9.921E+00	8.752E+01	0	0	0	0	0	0	-1.067E-10	0	-5.093E-05

(26)

Effective moduli determined by the FEM

1.596E+10	8.836E+09	8.616E+09	0	0	0	0	0	-1.510E-01	0	0	1.061E+01
8.836E+09	1.596E+10	8.616E+09	0	0	0	0	0	-1.511E-01	0	0	1.060E+01
8.616E+09	8.616E+09	8.333E+10	0	0	0	0	0	6.283E+00	0	0	8.749E+01
0	0	0	5.072E+09	0	0	0	0	9.842E-03	0	0	-1.790E-01
0	0	0	0	5.072E+09	0	0	9.815E-03	0	0	-1.795E-01	0
0	0	0	0	0	6.917E+09	0	0	0	0	0	0
0	0	0	0	9.815E-03	0	0	-1.716E-10	0	0	-2.689E-13	0
0	0	0	9.842E-03	0	0	0	0	-1.716E-10	0	0	-2.700E-13
-1.510E-01	-1.511E-01	6.283E+00	0	0	0	0	0	0	-3.869E-09	0	-1.169E-10
0	0	0	0	-1.795E-01	0	0	-2.689E-13	0	0	-3.137E-06	0
0	0	0	-1.790E-01	0	0	0	0	-2.702E-13	0	0	-3.136E-06
1.061E+01	1.060E+01	8.749E+01	0	0	0	0	0	0	-1.169E-10	0	-5.061E-05

(27)

Case (2)

Effective moduli determined by the Mori-Tanaka method

1.603E+10	7.770E+09	7.947E+09	0	0	0	1.055E-02	0	0	0	0	9.940E+00
7.770E+09	1.597E+10	8.292E+09	0	0	0	-2.522E-03	0	0	0	0	9.917E+00
7.947E+09	8.292E+09	8.627E+10	0	0	0	-4.410E-02	0	0	0	0	8.742E+01
0	0	0	4.616E+09	0	0	0	0	0	0	-1.436E-01	0
0	0	0	0	4.608E+09	0	0	0	4.625E-01	-1.578E-01	0	0
0	0	0	0	0	4.118E+09	0	7.370E-03	0	0	0	0
1.055E-02	-2.522E-03	-4.410E-02	0	0	0	-1.713E-10	0	0	0	0	3.027E-12
0	0	0	0	0	7.370E-03	0	-1.712E-10	0	0	0	0
0	0	0	0	4.625E-01	0	0	0	-4.303E-09	-1.241E-11	0	0
0	0	0	0	-1.578E-01	0	0	0	-1.241E-11	-3.410E-06	0	0
0	0	0	-1.436E-01	0	0	0	0	0	0	-3.008E-06	0
9.940E+00	9.917E+00	8.742E+01	0	0	0	3.027E-12	0	0	0	0	-4.943E-05

(28)

Effective moduli determined by the FEM

1.601E+10	8.829E+09	8.333E+09	0	0	0	9.426E-03	0	0	0	0	1.063E+01
8.830E+09	1.596E+10	8.611E+09	0	0	0	-1.216E-03	0	0	0	0	1.060E+01
8.333E+09	8.611E+09	8.602E+10	0	0	0	-4.439E-02	0	0	0	0	8.738E+01
0	0	0	5.014E+09	0	0	0	0	0	0	-1.780E-01	0
0	0	0	0	5.004E+09	0	0	0	5.167E-01	-1.992E-01	0	0
0	0	0	0	0	7.033E+09	0	1.501E-02	0	0	0	0
9.567E-03	-1.397E-03	-4.435E-02	0	0	0	-1.717E-10	0	0	0	0	2.928E-12
0	0	0	0	0	1.457E-02	0	-1.715E-10	0	0	0	0
0	0	0	0	5.170E-01	0	0	0	-4.265E-09	-1.664E-11	0	0
0	0	0	0	-1.937E-01	0	0	0	-1.606E-11	-3.609E-06	0	0
0	0	0	-1.722E-01	0	0	0	0	0	0	-3.145E-06	0
1.064E+01	1.061E+01	8.738E+01	0	0	0	2.975E-12	0	0	0	0	-4.912E-05

(29)

Case (3)

Effective moduli determined by the Mori-Tanaka method

1.594E+10	7.790E+09	8.400E+09	0	0	0	0	0	-1.413E-01	3.280E-01	0	0
7.790E+09	1.597E+10	8.304E+09	0	0	0	0	0	-1.414E-01	2.327E-01	0	0
8.400E+09	8.304E+09	8.715E+10	0	0	0	0	0	6.329E+00	8.501E-01	0	0
0	0	0	4.705E+09	0	0	0	0	8.891E-03	0	0	0
0	0	0	0	4.660E+09	0	0	9.102E-03	0	0	0	2.103E+01
0	0	0	0	0	4.057E+09	0	0	0	0	0	-1.196E-01
0	0	0	0	9.102E-03	0	0	-1.797E-10	0	0	0	3.225E-11
0	0	0	8.891E-03	0	0	0	0	-1.712E-10	0	0	0
-1.413E-01	-1.414E-01	6.329E+00	0	0	0	0	0	0	-3.890E-09	-3.014E-12	0
3.280E-01	2.327E-01	8.501E-01	0	0	0	0	0	0	-3.014E-12	-2.970E-06	0
0	0	0	0	0	-1.196E-01	0	0	0	0	0	-3.008E-06
0	0	0	0	2.103E+01	0	0	3.225E-11	0	0	0	1.717E-04

(30)

Effective moduli determined by the FEM

1.593E+10	8.828E+09	8.753E+09	0	0	0	0	0	-1.507E-01	3.609E-01	0	0
8.829E+09	1.595E+10	8.676E+09	0	0	0	0	0	-1.509E-01	2.740E-01	0	0
8.754E+09	8.676E+09	8.691E+10	0	0	0	0	0	6.281E+00	9.196E-01	0	0
0	0	0	5.131E+09	0	0	0	0	9.960E-03	0	0	0
0	0	0	0	5.074E+09	0	0	1.018E-02	0	0	0	2.362E+01
0	0	0	0	0	6.778E+09	0	0	0	0	0	-2.507E-01
0	0	0	0	1.018E-02	0	0	-1.800E-10	0	0	0	3.543E-11
0	0	0	9.967E-03	0	0	0	0	-1.718E-10	0	0	0
-1.508E-01	-1.510E-01	6.281E+00	0	0	0	0	0	0	-3.866E-09	-3.472E-12	0
3.663E-01	1.877E-01	8.906E-01	0	0	0	0	0	0	-2.546E-12	-3.089E-06	0
0	0	0	0	0	-2.965E-01	0	0	0	0	0	-3.141E-06
0	0	0	0	2.364E+01	0	0	3.543E-11	0	-0	0	1.706E-04

(31)

Case (4)

Effective moduli determined by the Mori-Tanaka method

1.597E+10	7.774E+09	8.342E+09	0	0	0	0	2.599E-03	0	0	-2.556E-01	0
7.774E+09	1.601E+10	8.095E+09	0	0	0	0	-1.086E-02	0	0	-3.615E-01	0
8.342E+09	8.095E+09	8.986E+10	0	0	0	0	4.539E-02	0	0	-9.294E-01	0
0	0	0	4.611E+09	0	0	0	0	-4.627E-01	0	0	-2.086E+01
0	0	0	0	4.662E+09	0	0	0	0	0	0	0
0	0	0	0	0	4.086E+09	-7.322E-03	0	0	1.203E-01	0	0
0	0	0	0	0	-7.322E-03	-1.712E-10	0	0	-1.804E-13	0	0
2.599E-03	-1.086E-02	4.539E-02	0	0	0	0	-1.799E-10	0	0	1.692E-13	0
0	0	0	-4.627E-01	0	0	0	0	-4.299E-09	0	0	1.639E-09
0	0	0	0	0	1.203E-01	-1.804E-13	0	0	-3.008E-06	0	0
-2.556E-01	-3.615E-01	-9.294E-01	0	0	0	0	1.692E-13	0	0	-3.364E-06	0
0	0	0	-2.086E+01	0	0	0	0	1.639E-09	0	0	1.732E-04

(32)

Effective moduli determined by the FEM

1.596E+10	8.833E+09	8.678E+09	0	0	0	0	1.194E-03	0	0	-3.058E-01	0
8.833E+09	1.600E+10	8.479E+09	0	0	0	0	-9.815E-03	0	0	-4.009E-01	0
8.678E+09	8.479E+09	8.961E+10	0	0	0	0	4.578E-02	0	0	-1.023E+00	0
0	0	0	5.011E+09	0	0	0	0	-5.187E-01	0	0	-2.334E+01
0	0	0	0	5.076E+09	0	0	0	0	0	0	0
0	0	0	0	0	6.904E+09	-1.478E-02	0	0	2.572E-01	0	0
0	0	0	0	0	-1.478E-02	-1.718E-10	0	0	-5.719E-13	0	0
1.194E-03	-9.815E-03	4.578E-02	0	0	0	0	-1.802E-10	0	0	6.887E-14	0
0	0	0	-5.187E-01	0	0	0	0	-4.261E-09	0	0	1.846E-09
0	0	0	0	0	2.572E-01	-5.719E-13	0	0	-3.150E-06	0	0
-3.058E-01	-4.009E-01	-1.023E+00	0	0	0	0	6.910E-14	0	0	-3.555E-06	0
0	0	0	-2.334E+01	0	0	0	0	1.846E-09	0	0	1.721E-04

(33)

Equations 26 and 27 are the effective matrix generated by Mori-Tanaka method and the FEM respectively. The direct comparison between the two is not reasonable because the FEM uses a specific symmetry arrangement of fibers that is not recognized by the Mori-Tanaka method. But the Mori-Tanaka method results are useful as a reference guidance.

In Case (1) and Case (4), where the piezoelectric phase and the piezomagnetic phase are poled to the same direction, $\langle E_1 \rangle$ is coupled with $\langle H_1 \rangle$ by the magnetoelectric constant λ_{11} . In the same way, $\langle E_2 \rangle$ and $\langle H_2 \rangle$ are coupled, $\langle E_3 \rangle$ and $\langle H_3 \rangle$ are coupled by λ_{11} and λ_{33} , respectively. In Case (2) and Case (3), by the effect of different poling directions, $\langle E_1 \rangle$ couples with $\langle H_3 \rangle$ and $\langle E_3 \rangle$ couples with $\langle H_1 \rangle$. In case (4), the magnitude of λ_{33} , which is coupled through ε_{23} , is one order larger than that of Case (1) which is coupled through ε_{31} .

Through the case study, we may note that we can control the coupling by changing the poling directions.

CHAPTER VI

CONCLUSIONS

The finite element method was used to solve an electro-magneto-elastic boundary value problem within a periodic unit cell of a fibrous composite and to determine the effective properties using periodicity boundary conditions. For a two-phase composite consisting of a piezomagnetic matrix reinforced with piezoelectric fibers, the effective properties as determined using the finite element method were in excellent agreement with the predictions of the Mori-Tanaka model of Li and Dunn (1998). The effective properties were also calculated for a three-phase composite consisting of piezoelectric and piezomagnetic fibers separated by an isotropic linear elastic matrix. The effective magnetoelectric moduli of this three-phase composite were about twenty times less than the magnetoelectric moduli of the two-phase composite because the epoxy matrix is not stiff enough to transfer significant strains between the piezomagnetic and piezoelectric fibers. Unlike the results for the two-phase composite, the effective moduli of the three-phase composite are not transversely isotropic even though the constituent phases are transversely isotropic. Through the parametric study, it was seen that the effective magnetoelectric coupling moduli are maximum when the piezoelectric volume fraction and the piezomagnetic volume fraction are roughly in a 1:1 ratio and then decrease as the matrix volume fraction increases. The differences between the finite element method results and the Mori-Tanaka results decrease as the matrix volume fraction increases.

The effective moduli are calculated and compared with Mori-Tanaka results for four different combinations of poling directions. It shows that we can control the coupling by changing the poling directions. Future work may include a systematic study of the effects of the following variables : the type of periodic unit cell, the shape of the phase, the stiffness of the elastic matrix.

REFERENCES

- [1] J. Y. Li and M. L. Dunn, "Micromechanics of Magnetoelastic Composite Materials: Average Fields and Effective Behavior", *Journal of Intelligent Material Systems and Structures*, vol. 9, pp. 404-416, June 1998.
- [2] J. Y. Li, "On micromechanics approximation for the effective thermoelastic moduli of multi-phase composite materials.", *Mechanics of Materials*, vol. 31, pp. 149-159, Feb. 1999.
- [3] J. Y. Li, "Magnetoelastic multi-inclusion and inhomogeneity problems and their applications in composite materials", *International Journal of Engineering Science*, vol. 38, pp. 1993-2011, Dec. 2000.
- [4] J. H. Huang and W. S. Kuo, "The analysis of piezoelectric/piezomagnetic composite materials containing ellipsoidal inclusions", *Journal of Applied Physics*, vol. 81, No. 3, pp. 1378-1386, Feb. 1997.
- [5] J. Y. Li and M. L. Dunn, "Anisotropic coupled-field inclusion and inhomogeneity problems", *Ph Magazine A*, vol. 77, No. 5, pp. 1341-1350, 1998.
- [6] J. Y. Li, M. L. Dunn, "Analysis of microstructural fields in heterogeneous piezoelectric solids", *International Journal of Engineering Science*, vol. 37, pp. 665-685, May 1999.
- [7] Y. Huang, K. X. Hu, X. Wei and A. Chandra, "A generalized self-consistent mechanics method for composite materials with multiphase inclusions", *J. Mech. Phys. Solids*, vol. 42, No. 3, pp. 491-504, Mar 1994.

- [8] J. Aboudi, "Micromechanical analysis of fully coupled electro-magneto-thermo-elastic multiphase composites", *Smart Materials and Structures*, vol. 10, pp. 867-877, Aug. 2001.
- [9] A.M.J.G Van Run, D.R Terrell, J.H. Scholing, "An in situ grown eutectic magnetoelectric composite material", *Journal of Material Science*, vol. 9, pp. 1710-1714, 1974.
- [10] C.W. Nan, "Magnetoelectric effect in composites of piezoelectric and piezomagnetic phases", *Physical Review B*, vol. 50, No. 22, pp. 6082-6088, Sept. 1994.
- [11] G. Harshe, J. P. Dougherty and R. E. Newnham, "Theoretical modeling of multilayer magnetoelectric composites", *International Journal of Applied Electromagnetics in Materials*, vol. 4, pp. 145-159, 1993.
- [12] Y. Benveniste, "Magnetoelectric effect in fibrous composites with piezoelectric and piezomagnetic phases", *Physical Review B*, vol. 51, No. 22, pp. 424-427, June 1995.
- [13] Y. Benveniste, "Exact Results in the Micromechanics of Fibrous Piezoelectric Composites Exhibiting Pyroelectricity", *Mathematical and Physical Sciences*, vol. 441, Issue 1911, pp. 59-81, Apr. 1993.
- [14] T. L. Wu and J. H. Huang, "Closed-form solutions for the magnetoelectric coupling coefficients in fibrous composites with piezoelectric and piezomagnetic phases", *International Journal of Solids and Structures*, vol. 37, pp. 2981-3009, May 2000.

- [15] J. H. Huang, H. K. Liu and W. L. Dai, "The optimized fiber volume fraction for magnetoelectric coupling effect in piezoelectric-piezomagnetic continuous fiber reinforced composites", *International Journal of Engineering Science*, vol. 38, pp. 1207-1217, July 2000.
- [16] J. G. Boyd, D. C. Lagoudas, and C. S. Seo, "Microscale Processing of Multifunctional Materials", 16th Annual Technical Conference American Society for Composites held at Virginia Tech, Blacksburg, Virginia, Sept. 10-12, 2001.
- [17] J. H. Huang, Y. H. Chiu, H. K. Liu, "Magneto-electro-elastic Eshelby tensors for a piezoelectric-piezomagnetic composite reinforced by ellipsoidal inclusions", *Journal of Applied Physics*, vol. 83, No. 10, pp. 5364-5370, May 1998.
- [18] M. Hori and S. Nemat-Nasser, "On two micromechanics theories for determining micro-macro relations in heterogeneous solids", *Mechanics of Materials*, vol. 31, pp. 667-682, Oct. 1999.
- [19] L. Pan, D. O. Adams and F. J. Rizzo, "Boundary element analysis for composite materials and a library of Green's functions", *Computers & Structures*, vol.66, pp. 685-693, 1998.
- [20] J. D. Whitcomb, C. D. Chapman and X. Tang, "Derivation of Boundary Conditions for Micromechanics Analyses of Plain and Satin Weave Composites", *Journal of Composite Materials*, vol. 34, pp. 724-747, 2000.
- [21] M. Kamiński, "Homogenized properties of periodic n-component composites", *International Journal of Engineering Science*, vol. 38, pp. 405-427, Mar. 2000.

- [22] S. Li, “General unit cells for micromechanical analyses of unidirectional composites”, *Composites Part A : Applied Science and Manufacturing*, vol. 32, pp. 815-826, June 2001.
- [23] C. T. Sun and R. S. Vaidya, “Prediction of composite properties from a representative volume element”, *Composites Science and Technology*, vol. 56, pp. 171-179, 1996.
- [24] J. D. Achenbach and H. Zhu, “Effect of interphases on micro and macromechanical behavior of hexagonal-array fiber composites”, *ASME Journal of Applied Mechanics*, vol. 57, pp. 956-963, Dec. 1990.
- [25] J. Schjødt-Thomsen, R. Pyrz, “The Mori-Tanaka stiffness tensor: diagonal symmetry, complex fibre orientations and non-dilute volume fractions”, *Mechanics of Materials*, vol. 33, pp. 531-544, Oct. 2001.
- [26] Y. Benveniste, G. J. Dvorak and T. Chen, “On diagonal and elastic symmetry of the approximate effective stiffness tensor of heterogeneous media”, *J. Mech. Phys. Solids*, vol. 39, No. 7, pp. 927-946, 1991.

APPENDIX A

FIELD PARTIAL DIFFERENTIAL EQUATIONS

The partial differential field equations for the piezoelectric phase and the piezomagnetic phase with x_3 as a symmetry axis are given by the following expressions

Piezoelectric

$$C_{11} \frac{\partial^2 u_1}{\partial x_1^2} + C_{66} \frac{\partial^2 u_1}{\partial x_2^2} + C_{44} \frac{\partial^2 u_1}{\partial x_3^2} + (C_{12} + C_{66}) \frac{\partial^2 u_2}{\partial x_1 \partial x_2} + (C_{13} + C_{44}) \frac{\partial^2 u_3}{\partial x_1 \partial x_3} + (e_{15} + e_{31}) \frac{\partial^2 \phi}{\partial x_1 \partial x_3} = 0 \quad (34)$$

$$C_{66} \frac{\partial^2 u_2}{\partial x_1^2} + C_{11} \frac{\partial^2 u_2}{\partial x_2^2} + C_{44} \frac{\partial^2 u_2}{\partial x_3^2} + (C_{12} + C_{66}) \frac{\partial^2 u_1}{\partial x_1 \partial x_2} + (C_{13} + C_{44}) \frac{\partial^2 u_3}{\partial x_2 \partial x_3} + (e_{15} + e_{31}) \frac{\partial^2 \phi}{\partial x_2 \partial x_3} = 0 \quad (35)$$

$$C_{44} \frac{\partial^2 u_3}{\partial x_1^2} + C_{44} \frac{\partial^2 u_3}{\partial x_2^2} + C_{33} \frac{\partial^2 u_3}{\partial x_3^2} + (C_{13} + C_{44}) \frac{\partial^2 u_1}{\partial x_1 \partial x_3} + (C_{13} + C_{44}) \frac{\partial^2 u_2}{\partial x_2 \partial x_3} + e_{15} \frac{\partial^2 \phi}{\partial x_1^2} + e_{15} \frac{\partial^2 \phi}{\partial x_2^2} + e_{33} \frac{\partial^2 \phi}{\partial x_3^2} = 0 \quad (36)$$

$$e_{15} \frac{\partial^2 u_3}{\partial x_1^2} + e_{15} \frac{\partial^2 u_3}{\partial x_2^2} + e_{33} \frac{\partial^2 u_3}{\partial x_3^2} + (e_{31} + e_{15}) \frac{\partial^2 u_1}{\partial x_1 \partial x_3} + (e_{31} + e_{15}) \frac{\partial^2 u_2}{\partial x_2 \partial x_3} - \eta_{11} \frac{\partial^2 \phi}{\partial x_1^2} - \eta_{11} \frac{\partial^2 \phi}{\partial x_2^2} - \eta_{33} \frac{\partial^2 \phi}{\partial x_3^2} = 0 \quad (37)$$

$$\mu_{11} \frac{\partial^2 \Phi}{\partial x_1^2} + \mu_{11} \frac{\partial^2 \Phi}{\partial x_2^2} + \mu_{33} \frac{\partial^2 \Phi}{\partial x_3^2} = 0 \quad (38)$$

Piezomagnetic

$$C_{11} \frac{\partial^2 u_1}{\partial x_1^2} + C_{66} \frac{\partial^2 u_1}{\partial x_2^2} + C_{44} \frac{\partial^2 u_1}{\partial x_3^2} + (C_{12} + C_{66}) \frac{\partial^2 u_2}{\partial x_1 \partial x_2} + (C_{13} + C_{44}) \frac{\partial^2 u_3}{\partial x_1 \partial x_3} + (q_{15} + q_{31}) \frac{\partial^2 \Phi}{\partial x_1 \partial x_3} = 0 \quad (39)$$

$$C_{66} \frac{\partial^2 u_2}{\partial x_1^2} + C_{11} \frac{\partial^2 u_2}{\partial x_2^2} + C_{44} \frac{\partial^2 u_2}{\partial x_3^2} + (C_{12} + C_{66}) \frac{\partial^2 u_1}{\partial x_1 \partial x_2} + (C_{13} + C_{44}) \frac{\partial^2 u_3}{\partial x_2 \partial x_3} + (q_{15} + q_{31}) \frac{\partial^2 \Phi}{\partial x_2 \partial x_3} = 0 \quad (40)$$

$$C_{44} \frac{\partial^2 u_3}{\partial x_1^2} + C_{44} \frac{\partial^2 u_3}{\partial x_2^2} + C_{33} \frac{\partial^2 u_3}{\partial x_3^2} + (C_{13} + C_{44}) \frac{\partial^2 u_1}{\partial x_1 \partial x_3} + (C_{13} + C_{44}) \frac{\partial^2 u_2}{\partial x_2 \partial x_3} + q_{15} \frac{\partial^2 \Phi}{\partial x_1^2} + q_{15} \frac{\partial^2 \Phi}{\partial x_2^2} + q_{33} \frac{\partial^2 \Phi}{\partial x_3^2} = 0 \quad (41)$$

$$q_{15} \frac{\partial^2 u_3}{\partial x_1^2} + q_{15} \frac{\partial^2 u_3}{\partial x_2^2} + q_{33} \frac{\partial^2 u_3}{\partial x_3^2} + (q_{31} + q_{15}) \frac{\partial^2 u_1}{\partial x_1 \partial x_3} + (q_{31} + q_{15}) \frac{\partial^2 u_2}{\partial x_2 \partial x_3} - \mu_{11} \frac{\partial^2 \Phi}{\partial x_1^2} - \mu_{11} \frac{\partial^2 \Phi}{\partial x_2^2} - \mu_{33} \frac{\partial^2 \Phi}{\partial x_3^2} = 0 \quad (42)$$

$$\eta_{11} \frac{\partial^2 \phi}{\partial x_1^2} + \eta_{11} \frac{\partial^2 \phi}{\partial x_2^2} + \eta_{33} \frac{\partial^2 \phi}{\partial x_3^2} = 0 \quad (43)$$

The field equations for the linear elastic matrix take the usual form (Lamé equations).

APPENDIX B

DIAGONAL SYMMETRY OF THE EFFECTIVE MODULI

The effective moduli of the three-phase electro-magneto-elastic composite are diagonally symmetry. In Appendix B, the diagonal symmetry of the effective moduli is proved.

The constitutive equations coupling the elastic, electric and magnetic fields are

$$\begin{aligned}\boldsymbol{\sigma} &= \mathbf{C}\boldsymbol{\varepsilon} - \mathbf{e}^T\mathbf{E} - \mathbf{q}^T\mathbf{H} \\ \mathbf{D} &= \mathbf{e}\boldsymbol{\varepsilon} + \boldsymbol{\eta}\mathbf{E} + \boldsymbol{\lambda}\mathbf{H} \\ \mathbf{B} &= \mathbf{q}\boldsymbol{\varepsilon} + \boldsymbol{\lambda}^T\mathbf{E} + \boldsymbol{\mu}\mathbf{H}\end{aligned}\quad (44)$$

To treat the elastic, electric and magnetic variables on equal footing, the constitutive equations coupling the elastic, electric and magnetic fields is compactly expressed in the following notation

$$\begin{pmatrix} \boldsymbol{\sigma} \\ \mathbf{D} \\ \mathbf{B} \end{pmatrix} = \begin{pmatrix} \mathbf{C} & \mathbf{e}^T & \mathbf{q}^T \\ \mathbf{e} & -\boldsymbol{\eta} & \boldsymbol{\lambda}^T \\ \mathbf{q} & \boldsymbol{\lambda} & -\boldsymbol{\mu} \end{pmatrix} \begin{pmatrix} \boldsymbol{\varepsilon} \\ -\mathbf{E} \\ -\mathbf{H} \end{pmatrix} \Leftrightarrow \boldsymbol{\Sigma} = \mathbf{L}\mathbf{Z} \quad (45)$$

$\boldsymbol{\Sigma}$, \mathbf{L} and \mathbf{Z} are (12x1),(12x12) and (12x1) matrix respectively.

This matrix notation can be expressed with index notation as

$$\Sigma_i = L_{ij}Z_j \quad i, j = 1, 2, 3, \dots, 12 \quad (46)$$

Each phase properties consisting the multi-phase composites satisfy the symmetry conditions

$$L_{ij}^{(n)} = L_{ji}^{(n)} \quad i, j = 1, 2, 3, \dots, 12 \quad (47)$$

In this paper, local fields will be denoted by an argument (x), and quantities without an argument will refer to averages.

Suppose that a representative volume V of a heterogeneous medium is subjected to two different states of uniform overall Z_j and Z'_j , the actual local fields are denoted as $\Sigma_i(x)$, $Z_j(x)$ and $\Sigma'_i(x)$, $Z'_j(x)$. They satisfy the following relationships.

$$\langle \Sigma_i(x) \rangle = \frac{1}{V} \int \Sigma_i(x) dV = \frac{1}{V} \int L_{ij}(x) Z_j(x) dV \quad (48)$$

$$\langle \Sigma'_i(x) \rangle = \frac{1}{V} \int \Sigma'_i(x) dV = \frac{1}{V} \int L_{ij}(x) Z'_j(x) dV \quad (49)$$

By the definition

$$\langle \Sigma_i(x) \rangle = L_{ij} \langle Z_j(x) \rangle \quad (50)$$

$$\langle \Sigma'_i(x) \rangle = L_{ij} \langle Z'_j(x) \rangle \quad (51)$$

Because $L_{ij}(x) = L_{ji}(x)$

$$\begin{aligned} \Sigma_i(x) Z'_i(x) &= L_{ij}(x) Z_j(x) Z'_i(x) \\ &= L_{ji}(x) Z'_i(x) Z_j(x) \\ &= \Sigma'_j(x) Z_j(x) \end{aligned} \quad (52)$$

so

$$\frac{1}{V} \int \Sigma_i(x) Z'_i(x) dV = \frac{1}{V} \int \Sigma'_j(x) Z_j(x) dV \quad (53)$$

$$\langle \Sigma_i(x) Z'_i(x) \rangle = \langle \Sigma'_j(x) Z_j(x) \rangle \quad (54)$$

By Hill-Mandel condition

$$\langle \Sigma_i(x) \rangle \langle Z'_i(x) \rangle = \langle \Sigma'_j(x) \rangle \langle Z_j(x) \rangle \quad (55)$$

$$L_{ij} \langle Z_j(x) \rangle \langle Z'_i(x) \rangle = L_{ji} \langle Z'_i(x) \rangle \langle Z_j(x) \rangle \quad (56)$$

$$L_{ij} = L_{ji} \quad (57)$$

There we have proved that the effective moduli is diagonally symmetric.

where the components of the tensor are given by

$$S_{1111} = \frac{a((3+2a)C_{11} + C_{12})}{2(1+a)^2 C_{11}} \quad (60) \quad S_{1122} = \frac{a((1+2a)C_{12} - C_{11})}{2(1+a)^2 C_{11}} \quad (61) \quad S_{1133} = \frac{aC_{13}}{(1+a)C_{11}} \quad (62)$$

$$S_{2211} = \frac{(2+a)C_{12} - aC_{11}}{2(1+a)^2 C_{11}} \quad (63) \quad S_{2222} = \frac{(2+3a)C_{11} + aC_{12}}{2(1+a)^2 C_{11}} \quad (64) \quad S_{2233} = \frac{C_{13}}{(1+a)C_{11}} \quad (65)$$

$$S_{2323} = \frac{1}{2(1+a)} \quad (66) \quad S_{1212} = \frac{(1+a+a^2)C_{11} - aC_{12}}{2(1+a)^2 C_{11}} \quad (67) \quad S_{1313} = \frac{a}{2(1+a)} \quad (68)$$

$$S_{1143} = \frac{ae_{31}}{(1+a)C_{11}} \quad (69) \quad S_{1153} = \frac{aq_{31}}{(1+a)C_{11}} \quad (70) \quad S_{2243} = \frac{e_{31}}{(1+a)C_{11}} \quad (71)$$

$$S_{2253} = \frac{q_{31}}{(1+a)C_{11}} \quad (71) \quad S_{4141} = \frac{a}{1+a} \quad (72) \quad S_{4242} = \frac{1}{1+a} \quad (73)$$

$$S_{5151} = \frac{a}{1+a} \quad (74) \quad S_{5252} = \frac{1}{1+a} \quad (75)$$

APPENDIX D

FEMLAB CODE

```

%%%%%%%%%%%%%%%%%%%%%%%%%%%%%%%%%%%%%%%%
% Three-phase 3-D model
% Three-phase composite consisting of epoxy resin matrix with piezoelectric and
% piezomagnetic cylindrical fiber
% solver : iterative solver
% element type : tetrahedron linear element
%%%%%%%%%%%%%%%%%%%%%%%%%%%%%%%%%%%%%%%%

clear all

tic
%%%%%%%%%%%%%%%%%%%%%%%%%%%%%%%%%%%%%%%%

casenum=input('Case number=');
% rotation angle for piezoelectric
theta_1=input('\nPiezoelectric rotation about x1 axis(1-2-3) = ');
theta_2=input('Piezoelectric rotation about x2 axis(1-2-3) = ');
theta_3=input('Piezoelectric rotation about x3 axis(1-2-3) = ');

theta1=theta_1*pi/180;
theta2=theta_2*pi/180;
theta3=theta_3*pi/180;

% rotation with x1 axis
R1e=[1,0,0;0,cos(theta1),sin(theta1);0,-sin(theta1),cos(theta1)];

% rotation with x2 axis
R2e=[cos(theta2),0,sin(theta2);0,1,0;-sin(theta2),0,cos(theta2)];

% rotation with x3 axis
R3e=[cos(theta3),sin(theta3),0;-sin(theta3),cos(theta3),0;0,0,1];

% total rotation tensor
Re=R3e*R2e*R1e;

% rotation angle for Piezomagnetic
theta_11=input('\nPiezomagnetic rotation about x1 axis(1-2-3) = ');
theta_22=input('Piezomagnetic rotation about x2 axis(1-2-3) = ');
theta_33=input('Piezomagnetic rotation about x3 axis(1-2-3) = ');

theta11=theta_11*pi/180;
theta22=theta_22*pi/180;
theta33=theta_33*pi/180;

% rotation with x1 axis
R1m=[1,0,0;0,cos(theta11),sin(theta11);0,-sin(theta11),cos(theta11)];

```

```

% rotation with x2 axis
R2m=[cos(theta22),0,sin(theta22);0,1,0;-sin(theta22),0,cos(theta22)];

% rotation with x3 axis
R3m=[cos(theta33),sin(theta33),0;-sin(theta33),cos(theta33),0;0,0,1];

% total rotation tensor
Rm=R3m*R2m*R1m;

% multiple factor for Epoxy Resin stiffness
mult=input('\nMultiple factor for Epoxy resin stiffness=');

for g=1:2
    if g==1

%% Piezoelectric with x3 poling (0,0,1)
% stiffness of piezomagnetic phase with x3 poling
C=[16.6,7.7,7.8,0,0,0;...
    7.7,16.6,7.8,0,0,0;...
    7.8,7.8,16.2,0,0,0;...
    0,0,4.3,0,0,0;...
    0,0,0,4.3,0,0;...
    0,0,0,0,4.45];
% piezomagnetic constant
e=[0,0,0,0,11.6,0;0,0,0,11.6,0,0;-4.4,-4.4,18.6,0,0,0];
% dielectroc constant
n=[112,0,0;0,112,0;0,0,126];
% magnetic constant
m=[5,0,0;0,5,0;0,0,10];
R=Re;

    elseif g==2
%% Piezomagnetic with x3 poling (0,0,1)
% stiffness of piezomagnetic phase with x3 poling
C=[28.6,17.3,17.05,0,0,0;...
    17.3,28.6,17.05,0,0,0;...
    17.05,17.05,26.95,0,0,0;...
    0,0,4.53,0,0,0;...
    0,0,0,4.53,0,0;...
    0,0,0,0,5.65];
% piezomagnetic constant
e=[0,0,0,0,5.5,0;0,0,0,5.5,0,0;5.803,5.803,6.997,0,0,0];
% dielectroc constant
n=[0.8,0,0;0,0.8,0;0,0,0.93];
% magnetic constant
m=[-590,0,0;0,-590,0;0,0,157];
R=Rm;
    end

```

```

% error estimate
for x=1:3
    for y=1:3
        if abs(R(x,y))<1e-5 R(x,y)=0;
        end
    end
end

%%%%%%%%%%%%%%
% rotation
%%%%%%%%%%%%%%

% mapping 6x6 matrix to 4th order tensor
L(1,1,1,1)=C(1,1);
L(1,1,2,2)=C(1,2); L(2,2,1,1)=C(1,2);
L(1,1,3,3)=C(1,3); L(3,3,1,1)=C(1,3);
L(1,1,2,3)=C(1,4); L(2,3,1,1)=C(1,4); L(1,1,3,2)=C(1,4); L(3,2,1,1)=C(1,4);
L(1,1,3,1)=C(1,5); L(3,1,1,1)=C(1,5); L(1,1,1,3)=C(1,5); L(1,3,1,1)=C(1,5);
L(1,1,1,2)=C(1,6); L(1,2,1,1)=C(1,6); L(1,1,2,1)=C(1,6); L(2,1,1,1)=C(1,6);

L(2,2,2,2)=C(2,2);
L(2,2,3,3)=C(2,3); L(3,3,2,2)=C(2,3);
L(2,2,2,3)=C(2,4); L(2,3,2,2)=C(2,4); L(2,2,3,2)=C(2,4); L(3,2,2,2)=C(2,4);
L(2,2,3,1)=C(2,5); L(3,1,2,2)=C(2,5); L(2,2,1,3)=C(2,5); L(1,3,2,2)=C(2,5);
L(2,2,1,2)=C(2,6); L(1,2,2,2)=C(2,6); L(2,2,2,1)=C(2,6); L(2,1,2,2)=C(2,6);

L(3,3,3,3)=C(3,3);
L(3,3,2,3)=C(3,4); L(2,3,3,3)=C(3,4); L(3,3,3,2)=C(3,4); L(3,2,3,3)=C(3,4);
L(3,3,3,1)=C(3,5); L(3,1,3,3)=C(3,5); L(3,3,1,3)=C(3,5); L(1,3,3,3)=C(3,5);
L(3,3,1,2)=C(3,6); L(1,2,3,3)=C(3,6); L(3,3,2,1)=C(3,6); L(2,1,3,3)=C(3,6);

L(2,3,2,3)=C(4,4); L(3,2,2,3)=C(4,4); L(2,3,3,2)=C(4,4); L(3,2,3,2)=C(4,4);
L(2,3,3,1)=C(4,5); L(3,2,3,1)=C(4,5); L(2,3,1,3)=C(4,5); L(3,2,1,3)=C(4,5);
L(3,1,2,3)=C(4,5); L(1,3,2,3)=C(4,5); L(3,1,3,2)=C(4,5); L(1,3,3,2)=C(4,5);
L(2,3,1,2)=C(4,6); L(3,2,1,2)=C(4,6); L(2,3,2,1)=C(4,6); L(3,2,2,1)=C(4,6);
L(1,2,2,3)=C(4,6); L(2,1,2,3)=C(4,6); L(1,2,3,2)=C(4,6); L(2,1,3,2)=C(4,6);

L(3,1,3,1)=C(5,5); L(1,3,3,1)=C(5,5); L(1,3,1,3)=C(5,5); L(3,1,1,3)=C(5,5);
L(3,1,1,2)=C(5,6); L(1,3,1,2)=C(5,6); L(3,1,2,1)=C(5,6); L(1,3,2,1)=C(5,6);
L(1,2,3,1)=C(5,6); L(2,1,3,1)=C(5,6); L(1,2,1,3)=C(5,6); L(2,1,1,3)=C(5,6);

L(1,2,1,2)=C(6,6); L(2,1,1,2)=C(6,6); L(1,2,2,1)=C(6,6); L(2,1,2,1)=C(6,6);

for i=1:3
    for j=1:3
        for k=1:3
            for l=1:3
                Lp(i,j,k,l)=0;
            end
        end
    end
end
end
for i=1:3

```

```

for j=1:3
  for k=1:3
    for l=1:3
      for p=1:3
        for q=1:3
          for r=1:3
            for s=1:3
              Lp(i,j,k,l)=Lp(i,j,k,l)+R(i,p)*R(j,q)*R(k,r)*R(l,s)*L(p,q,r,s);
            end
          end
        end
      end
    end
  end
end
end
end
end

```

```

% mapping 4th order tensor to 6x6 matrix

```

```

Cp(1,1)=Lp(1,1,1,1);
Cp(1,2)=Lp(1,1,2,2);
Cp(1,3)=Lp(1,1,3,3);
Cp(1,4)=Lp(1,1,2,3);
Cp(1,5)=Lp(1,1,3,1);
Cp(1,6)=Lp(1,1,1,2);

```

```

Cp(2,1)=Cp(1,2);
Cp(2,2)=Lp(2,2,2,2);
Cp(2,3)=Lp(2,2,3,3);
Cp(2,4)=Lp(2,2,2,3);
Cp(2,5)=Lp(2,2,3,1);
Cp(2,6)=Lp(2,2,1,2);

```

```

Cp(3,1)=Cp(1,3);
Cp(3,2)=Cp(2,3);
Cp(3,3)=Lp(3,3,3,3);
Cp(3,4)=Lp(3,3,2,3);
Cp(3,5)=Lp(3,3,3,1);
Cp(3,6)=Lp(3,3,1,2);

```

```

Cp(4,1)=Cp(1,4);
Cp(4,2)=Cp(2,4);
Cp(4,3)=Cp(3,4);
Cp(4,4)=Lp(2,3,2,3);
Cp(4,5)=Lp(2,3,3,1);
Cp(4,6)=Lp(2,3,1,2);

```

```

Cp(5,1)=Cp(1,5);Cp(5,2)=Cp(2,5);Cp(5,3)=Cp(3,5);Cp(5,4)=Cp(4,5);
Cp(5,5)=Lp(3,1,3,1);
Cp(5,6)=Lp(3,1,1,2);

```

```

Cp(6,1)=Cp(1,6);Cp(6,2)=Cp(2,6);Cp(6,3)=Cp(3,6);Cp(6,4)=Cp(4,6);Cp(6,5)=Cp(5,6);
Cp(6,6)=Lp(1,2,1,2);

```



```

%%%%%%%%%%
% 3rd order tensor
%%%%%%%%%%
% mapping 3x6 matrix to 3rd order tensor

T(1,1,1)=e(1,1);T(1,1,2)=e(1,6);T(1,1,3)=e(1,5);
T(1,2,1)=e(1,6);T(1,2,2)=e(1,2);T(1,2,3)=e(1,4);
T(1,3,1)=e(1,5);T(1,3,2)=e(1,4);T(1,3,3)=e(1,3);

T(2,1,1)=e(2,1);T(2,1,2)=e(2,6);T(2,1,3)=e(2,5);
T(2,2,1)=e(2,6);T(2,2,2)=e(2,2);T(2,2,3)=e(2,4);
T(2,3,1)=e(2,5);T(2,3,2)=e(2,4);T(2,3,3)=e(2,3);

T(3,1,1)=e(3,1);T(3,1,2)=e(3,6);T(3,1,3)=e(3,5);
T(3,2,1)=e(3,6);T(3,2,2)=e(3,2);T(3,2,3)=e(3,4);
T(3,3,1)=e(3,5);T(3,3,2)=e(3,4);T(3,3,3)=e(3,3);

for i=1:3
    for j=1:3
        for k=1:3
            Tp(i,j,k)=0;
        end
    end
end

for i=1:3
    for j=1:3
        for k=1:3
            for p=1:3
                for q=1:3
                    for r=1:3
                        Tp(i,j,k)=Tp(i,j,k)+R(i,p)*R(j,q)*R(k,r)*T(p,q,r);
                    end
                end
            end
        end
    end
end

% mapping 3rd order tensor to 3x6 matrix
ep(1,1)=Tp(1,1,1);ep(1,2)=Tp(1,2,2);ep(1,3)=Tp(1,3,3);ep(1,4)=Tp(1,2,3);ep(1,5)=Tp(1,3,1);ep(1,6)=Tp(1,1,2);
ep(2,1)=Tp(2,1,1);ep(2,2)=Tp(2,2,2);ep(2,3)=Tp(2,3,3);ep(2,4)=Tp(2,2,3);ep(2,5)=Tp(2,3,1);ep(2,6)=Tp(2,1,2);
ep(3,1)=Tp(3,1,1);ep(3,2)=Tp(3,2,2);ep(3,3)=Tp(3,3,3);ep(3,4)=Tp(3,2,3);ep(3,5)=Tp(3,3,1);ep(3,6)=Tp(3,1,2);

%%%%%%%%%%
% 2nd order tensor
%%%%%%%%%%
np=zeros(3,3);

for i=1:3

```

```

    for j=1:3
        for p=1:3
            for q=1:3
                np(i,j)=np(i,j)+R(i,p)*R(j,q)*n(p,q);
            end
        end
    end
end

mp=zeros(3,3);
for i=1:3
    for j=1:3
        for p=1:3
            for q=1:3
                mp(i,j)=mp(i,j)+R(i,p)*R(j,q)*m(p,q);
            end
        end
    end
end

if g==1
    C_e=Cp;
    e_e=ep;
    n_e=np;
    m_e=mp;
elseif g==2
    C_m=Cp;
    q_m=ep;
    n_m=np;
    m_m=mp;
end

end

% input volume percent of piezomagnetic and piezoelectric phase
V1=input('\n Volume percent of piezomagnetic circular cylindrical phase = ');
V2=input('Volume percent of piezoelectric circular cylindrical phase = ');
% calculate radius of each phase : r1=piezomagnetic, r2=piezoelectric
r1=sqrt(V1/pi);
r2=sqrt(V2/pi);
% mesh type
a=input('\n choose the number of initial mesh type : \n 1=extra coarse \n 2=coarser \n 3=coarse \n
4=normal \n 5=fine \n 6=finer \n \n Your mesh type = ');
if a==1
    h1=0.8;h2=0.04;h3=1.8;h4=3;b='extracoarse';
elseif a==2
    h1=0.6;h2=0.03;h3=1.6;h4=1.9;b='coarser';
elseif a==3
    h1=0.5;h2=0.02;h3=1.5;h4=1.5;b='coarse';
elseif a==4
    h1=0.4;h2=0.01;h3=1.4;h4=1;b='normal';
elseif a==5
    h1=0.37;h2=0.009;h3=1.35;h4=0.9;b='fine';

```

```

elseif a==6
    h1=0.3;h2=0.005;h3=1.35;h4=0.55;b='finer';
end

%SOLVER TYPE
z=input("\n choose the number of solver type: \n 1=normal solver \n 2=iterative solver \n \n Your choice
= ');

% 12 boundary conditions
for i=1:12;
i
t0=clock;
starttime=fix(clock)

flclear fem
% FEMLAB Version
clear vrsn;
vrsn.name='FEMLAB 2.3';
vrsn.major=0;
vrsn.build=148;
fem.version=vrsn;

% Recorded command sequence

% New geometry 1
fem.sdim={'x','y','z'};

% Geometry
% Center Circle and rectangular
Co=circ2(5,5,r1,0);
Ro=rect2(0,10,0,10,0);
% left down 1/4 circle
R1=rect2(0,10,0,10,0);
C1=circ2(0,0,r2,0);
Co1=R1*C1;
% rotate 1/4 circle
Co2=rotate(Co1,90*(pi/180),5,5);
Co3=rotate(Co2,90*(pi/180),5,5);
Co4=rotate(Co3,90*(pi/180),5,5);
% make 2D coerce composite
g1=geomcoerce('solid', {Co1,Co2,Co3,Co4,Co,Ro});
% extrude
g2=extrude(g1,'Distance',10,'Scale',[1;1],'Displ',[0;0],'Wrkpln',[0 1 0;0 0 1;0 0 0]);
% put a point in
v=point3(5,5,5);
g3=geomcoerce('solid', {g2 v});

clear s f c p
objs={g3};
name={'EXT1'};
s.objs=objs;
s.name=name;

```

```

objs={};
name={};
f.objs=objs;
f.name=name;

objs={};
name={};
c.objs=objs;
c.name=name;

objs={};
name={};
p.objs=objs;
p.name=name;

drawstruct=struct('s','f','c','p');
fem.draw=drawstruct;
fem.geom=geomcsg(fem);

clear appl

% Application mode 1
appl{1}.mode=flpdec3d(5,'dim',{'u','v','w','V','M','u_t','v_t','w_t','V_t', ...
'M_t'},'sdim',{'x','y','z'},'submode','std','tdiff','on');
appl{1}.dim={'u','v','w','V','M','u_t','v_t','w_t','V_t','M_t'};
appl{1}.form='coefficient';
appl{1}.border='off';
appl{1}.name='c1';
appl{1}.var={};
appl{1}.assign={'abscu1x','abscu1x','abscu2x','abscu2x','abscu3x','abscu3x'; ...
'abscu4x','abscu4x','abscu5x','abscu5x','absga1x','absga1x','absga2x'; ...
'absga2x','absga3x','absga3x','absga4x','absga4x','absga5x','absga5x'; ...
'absu1x','absux','absu2x','absvx','absu3x','abswx','absu4x','absVx'; ...
'absu5x','absMx'};
appl{1}.elemdefault='Lag2';
appl{1}.shape={'shlag(1,"u'),'shlag(1,"v'),'shlag(1,"w)', ...
'shlag(1,"V'),'shlag(1,"M'),'shlag(2,"u'),'shlag(2,"v)', ...
'shlag(2,"w'),'shlag(2,"V'),'shlag(2,"M)'};
appl{1}.sshape=1;
appl{1}.equ.da={{'1','0','0','0','0','0','0','1','0','0', ...
'0','0','0','1','0','0','0','0','0','1','0','0', ...
'0','0','0','1'}};
appl{1}.equ.c={{'1','0','0','0','0','0','0','1','0','0', ...
'0','0','1','0','0','0','0','0','1','0','0','0', ...
'0','0','1'}};
appl{1}.equ.al={{'0','0','0','0','0','0','0','0','0', ...
'0','0','0','0','0','0','0','0','0','0', ...
'0','0','0','0','0','0','0','0','0','0', ...
'0','0','0','0','0','0','0','0','0','0', ...
'0','0','0','0','0','0','0','0','0','0'}};
appl{1}.equ.ga={{'0','0','0','0','0','0','0','0','0', ...
'0','0','0'}};

```

```

appl{1}.equ.be={{{'0';'0';'0'},{'0';'0';'0'},{'0';'0';'0'},{'0';'0';'0'}, ...
{'0';'0';'0'},{'0';'0';'0'},{'0';'0';'0'},{'0';'0';'0'},{'0';'0';'0'},{'0'; ...
'0';'0'},{'0';'0';'0'},{'0';'0';'0'},{'0';'0';'0'},{'0';'0';'0'},{'0';'0'; ...
'0'},{'0';'0';'0'},{'0';'0';'0'},{'0';'0';'0'},{'0';'0';'0'},{'0';'0';'0'; ...
{'0';'0';'0'},{'0';'0';'0'},{'0';'0';'0'},{'0';'0';'0'},{'0';'0';'0'}}};
appl{1}.equ.a={{{'0'},{'0'},{'0'},{'0'},{'0'},{'0'},{'0'},{'0'},{'0'},{'0'}; ...
{'0'},{'0'},{'0'},{'0'},{'0'},{'0'},{'0'},{'0'},{'0'},{'0'},{'0'}, ...
{'0'},{'0'},{'0'}}};
appl{1}.equ.f={{{'1'},{'1'},{'1'},{'1'},{'1'}}};
appl{1}.equ.weak={{{'0'},{'0'},{'0'},{'0'},{'0'}}};
appl{1}.equ.dweak={{{'0'},{'0'},{'0'},{'0'},{'0'}}};
appl{1}.equ.constr={{{'0'},{'0'},{'0'},{'0'},{'0'}}};
appl{1}.equ.gporder={{4;4;4;4;4}};
appl{1}.equ.cporder={{2;2;2;2;2}};
appl{1}.equ.shape={6;10};
appl{1}.equ.init={{{'0'},{'0'},{'0'},{'0'},{'0'}}};
appl{1}.equ.usage={1};
appl{1}.equ.ind=ones(1,6);
appl{1}.bnd.q={{{'0'},{'0'},{'0'},{'0'},{'0'},{'0'},{'0'},{'0'},{'0'},{'0'}; ...
{'0'},{'0'},{'0'},{'0'},{'0'},{'0'},{'0'},{'0'},{'0'},{'0'},{'0'}, ...
{'0'},{'0'},{'0'},{'0'},{'0'},{'0'},{'0'},{'0'},{'0'},{'0'},{'0'}, ...
{'0'},{'0'},{'0'},{'0'},{'0'},{'0'},{'0'},{'0'},{'0'},{'0'},{'0'}, ...
{'0'},{'0'},{'0'},{'0'}}};
appl{1}.bnd.g={{{'0'},{'0'},{'0'},{'0'},{'0'},{'0'},{'0'},{'0'},{'0'}, ...
{'0'}}};
appl{1}.bnd.h={{{'1'},{'0'},{'0'},{'0'},{'0'},{'0'},{'1'},{'0'},{'0'},{'0'}; ...
{'0'},{'0'},{'1'},{'0'},{'0'},{'0'},{'0'},{'0'},{'1'},{'0'},{'0'},{'0'}, ...
{'0'},{'0'},{'1'},{'0'},{'0'},{'0'},{'0'},{'0'},{'1'},{'0'},{'0'},{'0'}, ...
{'0'},{'0'},{'0'},{'1'},{'0'},{'0'},{'0'},{'0'},{'0'},{'1'},{'0'},{'0'}, ...
{'0'},{'0'},{'0'},{'1'}}};
appl{1}.bnd.r={{{'0'},{'0'},{'0'},{'0'},{'0'},{'0'},{'0'},{'0'},{'0'}, ...
{'0'}}};
appl{1}.bnd.type='dir','neu';
appl{1}.bnd.weak={{{'0'},{'0'},{'0'},{'0'},{'0'},{'0'},{'0'},{'0'},{'0'}, ...
{'0'}}};
appl{1}.bnd.dweak={{{'0'},{'0'},{'0'},{'0'},{'0'},{'0'},{'0'},{'0'},{'0'}, ...
{'0'}}};
appl{1}.bnd.constr={{{'0'},{'0'},{'0'},{'0'},{'0'},{'0'},{'0'},{'0'}, ...
{'0'},{'0'}}};
appl{1}.bnd.gporder={{0;0;0;0;0},{0;0;0;0;0}};
appl{1}.bnd.cporder={{0;0;0;0;0},{0;0;0;0;0}};
appl{1}.bnd.shape={0,0};
appl{1}.bnd.ind=[1 1 1 1 2 1 1 2 1 1 2 1 1 2 2 1 1 1 2 2 1 1 2 1 1 2 1 1 1 ...
1 1 1];
appl{1}.edg.weak={{{'0'},{'0'},{'0'},{'0'},{'0'}}};
appl{1}.edg.dweak={{{'0'},{'0'},{'0'},{'0'},{'0'}}};
appl{1}.edg.constr={{{'0'},{'0'},{'0'},{'0'},{'0'}}};
appl{1}.edg.gporder={{0;0;0;0;0}};
appl{1}.edg.cporder={{0;0;0;0;0}};
appl{1}.edg.shape={0};
appl{1}.edg.ind=ones(1,56);
appl{1}.pnt.weak={{{'0'},{'0'},{'0'},{'0'},{'0'}}};
appl{1}.pnt.dweak={{{'0'},{'0'},{'0'},{'0'},{'0'}}};

```

```

appl{1}.pnt.constr={{{'0'}};{'0'}};{'0'}};{'0'}};{'0'}};
appl{1}.pnt.shape={0};
appl{1}.pnt.ind=ones(1,33);

fem.appl=appl;

% Symmetry boundaries
fem.equiv=[1 5 9 2 18 22 3 7 24 28 16 11;30 31 32 13 19 27 4 8 25 29 17 12];

% Initialize mesh
fem.mesh=meshinit(fem,...
    'Out', {'mesh'},...
    'jiggle', 'on',...
    'Hcurve', h1,...
    'Hcutoff',h2,...
    'Hgrad', h3,...
    'Hmaxfact',h4,...
    'Hmax', {[],zeros(1,0),zeros(1,0),zeros(1,0),zeros(1,0)});

% Differentiation rules
fem.rules={};

% Problem form
fem.outform='coefficient';

% Geometry element order
fem.outsshape=1;

% Differentiation
fem.diff={'expr'};

% Differentiation simplification
fem.simplify='on';

% Point settings
clear pnt
pnt.weak={{{'0'}};{'0'}};{'0'}};{'0'}};{'0'}};{'0'}};{'0'}};{'0'}};{'0'}};{'0'}};
pnt.dweak={{{'0'}};{'0'}};{'0'}};{'0'}};{'0'}};{'0'}};{'0'}};{'0'}};{'0'}};{'0'}};
pnt.constr={{{'0'}};{'0'}};{'0'}};{'0'}};{'0'}};{'0-u'}};{'0-v'}};{'0-w'}}; ...
{'0-V'}};{'0-M'}};};
pnt.shape={0,0};
pnt.ind=[1 1 1 1 1 1 1 1 1 1 1 1 1 1 1 1 2 1 1 1 1 1 1 1 1 1 1 1 1 1 1 1];
fem.appl{1}.pnt=pnt;

% Edge settings
clear edg
edg.weak={{{'0'}};{'0'}};{'0'}};{'0'}};{'0'}};};
edg.dweak={{{'0'}};{'0'}};{'0'}};{'0'}};{'0'}};};
edg.constr={{{'0'}};{'0'}};{'0'}};{'0'}};{'0'}};};
edg.gporder={{0,0;0,0;0,0}};
edg.cporder={{0,0;0,0;0,0}};

```



```

{'0';{'0';{'0';{'0';{'0';{'1'}};{'1';{'0';{'0';{'0';{'0';{'0'}}, ...
{'1';{'0';{'0';{'0';{'0';{'0';{'0';{'0';{'0';{'0';{'0'}}, ...
{'1';{'0';{'0';{'0';{'0';{'0';{'0';{'1'}};{'-1';{'0';{'0';{'0';{'0'}}, ...
{'0';{'-1';{'0';{'0';{'0';{'0';{'0';{'0';{'-1';{'0';{'0';{'0';{'0'}}, ...
{'0';{'-1';{'0';{'0';{'0';{'0';{'0';{'0';{'-1'}};{'-1';{'0';{'0'}}, ...
{'0';{'0';{'0';{'-1';{'0';{'0';{'0';{'0';{'0';{'-1';{'0';{'0'}}, ...
{'0';{'0';{'0';{'-1';{'0';{'0';{'0';{'0';{'0';{'-1'}};{'1';{'0'}}, ...
{'0';{'0';{'0';{'0';{'1';{'0';{'0';{'0';{'0';{'0';{'1';{'0'}}, ...
{'0';{'0';{'0';{'0';{'1';{'0';{'0';{'0';{'0';{'0';{'1'}};{'-1'}}, ...
{'0';{'0';{'0';{'0';{'0';{'-1';{'0';{'0';{'0';{'0';{'0';{'-1'}}, ...
{'0';{'0';{'0';{'0';{'0';{'-1';{'0';{'0';{'0';{'0';{'0';{'-1'}}}, ...
{'-1';{'0';{'0';{'0';{'0';{'0';{'0';{'-1';{'0';{'0';{'0';{'0'}}, ...
{'-1'};{'-1';{'0';{'0';{'0';{'0';{'0';{'-1';{'0';{'0';{'0';{'0'}}, ...
{'0';{'0';{'-1';{'0';{'0';{'0';{'0';{'0';{'-1';{'0';{'0';{'0'}}, ...
{'0';{'0';{'-1'}};{'-1';{'0';{'0';{'0';{'0';{'0';{'-1';{'0'}}, ...
{'0';{'0';{'0';{'0';{'-1';{'0';{'0';{'0';{'0';{'0';{'-1';{'0'}}, ...
{'0';{'0';{'0';{'0';{'-1'}}};
if i==1
bnd.r={{{'-0.01';{'0';{'0';{'0';{'0'}},...%boundary 1 x=0
{'0';{'0';{'0';{'0';{'0'}}, ...%boundary 2 y=0
{'0';{'0';{'0';{'0';{'0'}},...%boundary 3 z=0
{'0';{'0';{'0';{'0';{'0'}},...%boundary 4 z=10
{'-0.01';{'0';{'0';{'0';{'0'}},...%boundary 5 x=0
{'0';{'0';{'0';{'0';{'0'}},...%boundary
{'0';{'0';{'0';{'0';{'0'}},...%boundary 7 z=0
{'0';{'0';{'0';{'0';{'0'}},...%boundary 8 z=10
{'-0.01';{'0';{'0';{'0';{'0'}},...%boundary 9 x=0
{'0';{'0';{'0';{'0';{'0'}},...%boundary 11 z=0
{'0';{'0';{'0';{'0';{'0'}},...%boundary 12 z=10
{'0';{'0';{'0';{'0';{'0'}},...%boundary 13 y=10
{'0';{'0';{'0';{'0';{'0'}},...%boundary 16 z=0
{'0';{'0';{'0';{'0';{'0'}},...%boundary 17 z=10
{'0';{'0';{'0';{'0';{'0'}},...%boundary 18 y=0
{'0';{'0';{'0';{'0';{'0'}},...%boundary 19 y=10
{'0';{'0';{'0';{'0';{'0'}},...%boundary 22 y=0
{'0';{'0';{'0';{'0';{'0'}},...%boundary 24 z=0
{'0';{'0';{'0';{'0';{'0'}},...%boundary 25 z=10
{'0';{'0';{'0';{'0';{'0'}},...%boundary 27 y=10
{'0';{'0';{'0';{'0';{'0'}},...%boundary 28 z=0
{'0';{'0';{'0';{'0';{'0'}},...%boundary 29 z=10
{'0';{'0';{'0';{'0';{'0'}},...%boundary 30 x=10
{'0';{'0';{'0';{'0';{'0'}},...%boundary 31 x=10
{'0';{'0';{'0';{'0';{'0'}},...%boundary 32 x=10
elseif i==2
bnd.r={{{'0';{'0';{'0';{'0';{'0'}},...%boundary 1 x=0
{'0';{'-0.01';{'0';{'0';{'0'}}, ...%boundary 2 y=0
{'0';{'0';{'0';{'0';{'0'}},...%boundary 3 z=0
{'0';{'0';{'0';{'0';{'0'}},...%boundary 4 z=10
{'0';{'0';{'0';{'0';{'0'}},...%boundary 5 x=10
{'0';{'0';{'0';{'0';{'0'}},...%boundary
{'0';{'0';{'0';{'0';{'0'}},...%boundary 7 z=0
{'0';{'0';{'0';{'0';{'0'}},...%boundary 8 z=10

```

```

{{'0';{'0';{'0';{'0';{'0'}}},...%boundary 9 x=0
{{'0';{'0';{'0';{'0';{'0'}}},...%boundary 11 z=0
{{'0';{'0';{'0';{'0';{'0'}}},...%boundary 12 z=10
{{'0';{'0';{'0';{'0';{'0'}}},...%boundary 13 y=10
{{'0';{'0';{'0';{'0';{'0'}}},...%boundary 16 z=0
{{'0';{'0';{'0';{'0';{'0'}}},...%boundary 17 z=10
{{'0';{'-0.01';{'0';{'0';{'0'}}},...%boundary 18 y=0
{{'0';{'0';{'0';{'0';{'0'}}},...%boundary 19 y=10
{{'0';{'-0.01';{'0';{'0';{'0'}}},...%boundary 22 y=0
{{'0';{'0';{'0';{'0';{'0'}}},...%boundary 24 z=0
{{'0';{'0';{'0';{'0';{'0'}}},...%boundary 25 z=10
{{'0';{'0';{'0';{'0';{'0'}}},...%boundary 27 y=10
{{'0';{'0';{'0';{'0';{'0'}}},...%boundary 28 z=0
{{'0';{'0';{'0';{'0';{'0'}}},...%boundary 29 z=10
{{'0';{'0';{'0';{'0';{'0'}}},...%boundary 30 x=10
{{'0';{'0';{'0';{'0';{'0'}}},...%boundary 31 x=10
{{'0';{'0';{'0';{'0';{'0'}}},...%boundary 32 x=10
elseif i==3
bnd.r={{'0';{'0';{'0';{'0';{'0'}}},...%boundary 1 x=0
{{'0';{'0';{'0';{'0';{'0'}}}, ...%boundary 2 y=0
{{'0';{'0';{'-0.01';{'0';{'0'}}},...%boundary 3 z=0
{{'0';{'0';{'0';{'0';{'0'}}},...%boundary 4 z=10
{{'0';{'0';{'0';{'0';{'0'}}},...%boundary 5 x=10
{{'0';{'0';{'0';{'0';{'0'}}},...%boundary
{{'0';{'0';{'-0.01';{'0';{'0'}}},...%boundary 7 z=0
{{'0';{'0';{'0';{'0';{'0'}}},...%boundary 8 z=10
{{'0';{'0';{'0';{'0';{'0'}}},...%boundary 9 x=0
{{'0';{'0';{'-0.01';{'0';{'0'}}},...%boundary 11 z=0
{{'0';{'0';{'0';{'0';{'0'}}},...%boundary 12 z=10
{{'0';{'0';{'0';{'0';{'0'}}},...%boundary 13 y=10
{{'0';{'0';{'-0.01';{'0';{'0'}}},...%boundary 16 z=0
{{'0';{'0';{'0';{'0';{'0'}}},...%boundary 17 z=10
{{'0';{'0';{'0';{'0';{'0'}}},...%boundary 18 y=0
{{'0';{'0';{'0';{'0';{'0'}}},...%boundary 19 y=10
{{'0';{'0';{'0';{'0';{'0'}}},...%boundary 22 y=0
{{'0';{'0';{'-0.01';{'0';{'0'}}},...%boundary 24 z=0
{{'0';{'0';{'0';{'0';{'0'}}},...%boundary 25 z=10
{{'0';{'0';{'0';{'0';{'0'}}},...%boundary 27 y=10
{{'0';{'0';{'-0.01';{'0';{'0'}}},...%boundary 28 z=0
{{'0';{'0';{'0';{'0';{'0'}}},...%boundary 29 z=10
{{'0';{'0';{'0';{'0';{'0'}}},...%boundary 30 x=10
{{'0';{'0';{'0';{'0';{'0'}}},...%boundary 31 x=10
{{'0';{'0';{'0';{'0';{'0'}}},...%boundary 32 x=10
elseif i==4
bnd.r={{'0';{'0';{'0';{'0';{'0'}}},...%boundary 1 x=0
{{'0';{'0';{'0';{'0';{'0'}}}, ...%boundary 2 y=0
{{'0';{'-0.005';{'0';{'0';{'0'}}},...%boundary 3 z=0
{{'0';{'-0.005';{'0';{'0';{'0'}}},...%boundary 4 z=10
{{'0';{'0';{'0';{'0';{'0'}}},...%boundary 5 x=10
{{'0';{'0';{'0';{'0';{'0'}}},...%boundary
{{'0';{'-0.005';{'0';{'0';{'0'}}},...%boundary 7 z=0
{{'0';{'-0.005';{'0';{'0';{'0'}}},...%boundary 8 z=10
{{'0';{'0';{'0';{'0';{'0'}}},...%boundary 9 x=0

```

```

{{'0';{'-0.005';{'0';{'0';{'0'}}},...%boundary 11 z=0
{{'0';{'-0.005';{'0';{'0';{'0'}}},...%boundary 12 z=10
{{'0';{'0';{'0';{'0';{'0'}}},...%boundary 13 y=10
{{'0';{'-0.005';{'0';{'0';{'0'}}},...%boundary 16 z=0
{{'0';{'-0.005';{'0';{'0';{'0'}}},...%boundary 17 z=10
{{'0';{'0';{'0';{'0';{'0'}}},...%boundary 18 y=0
{{'0';{'0';{'0';{'0';{'0'}}},...%boundary 19 y=10
{{'0';{'0';{'0';{'0';{'0'}}},...%boundary 22 y=0
{{'0';{'-0.005';{'0';{'0';{'0'}}},...%boundary 24 z=0
{{'0';{'-0.005';{'0';{'0';{'0'}}},...%boundary 25 z=10
{{'0';{'0';{'0';{'0';{'0'}}},...%boundary 27 y=10
{{'0';{'-0.005';{'0';{'0';{'0'}}},...%boundary 28 z=0
{{'0';{'-0.005';{'0';{'0';{'0'}}},...%boundary 29 z=10
{{'0';{'0';{'0';{'0';{'0'}}},...%boundary 30 x=10
{{'0';{'0';{'0';{'0';{'0'}}},...%boundary 31 x=10
{{'0';{'0';{'0';{'0';{'0'}}},...%boundary 32 x=10
elseif i==5
bnd.r={{'0';{'0';{'-0.005';{'0';{'0'}}},...%boundary 1 x=0
{{'0';{'0';{'0';{'0';{'0'}}}, ...%boundary 2 y=0
{{'0';{'0';{'0';{'0';{'0'}}},...%boundary 3 z=0
{{'0';{'0';{'0';{'0';{'0'}}},...%boundary 4 z=10
{{'0';{'0';{'-0.005';{'0';{'0'}}},...%boundary 5 x=0
{{'0';{'0';{'0';{'0';{'0'}}},...%boundary
{{'0';{'0';{'0';{'0';{'0'}}},...%boundary 7 z=0
{{'0';{'0';{'0';{'0';{'0'}}},...%boundary 8 z=10
{{'0';{'0';{'-0.005';{'0';{'0'}}},...%boundary 9 x=0
{{'0';{'0';{'0';{'0';{'0'}}},...%boundary 11 z=0
{{'0';{'0';{'0';{'0';{'0'}}},...%boundary 12 z=10
{{'0';{'0';{'0';{'0';{'0'}}},...%boundary 13 y=10
{{'0';{'0';{'0';{'0';{'0'}}},...%boundary 16 z=0
{{'0';{'0';{'0';{'0';{'0'}}},...%boundary 17 z=10
{{'0';{'0';{'0';{'0';{'0'}}},...%boundary 18 y=0
{{'0';{'0';{'0';{'0';{'0'}}},...%boundary 19 y=10
{{'0';{'0';{'0';{'0';{'0'}}},...%boundary 22 y=0
{{'0';{'0';{'0';{'0';{'0'}}},...%boundary 24 z=0
{{'0';{'0';{'0';{'0';{'0'}}},...%boundary 25 z=10
{{'0';{'0';{'0';{'0';{'0'}}},...%boundary 27 y=10
{{'0';{'0';{'0';{'0';{'0'}}},...%boundary 28 z=0
{{'0';{'0';{'0';{'0';{'0'}}},...%boundary 29 z=10
{{'0';{'0';{'-0.005';{'0';{'0'}}},...%boundary 30 x=10
{{'0';{'0';{'-0.005';{'0';{'0'}}},...%boundary 31 x=10
{{'0';{'0';{'-0.005';{'0';{'0'}}},...%boundary 32 x=10
elseif i==6
bnd.r={{'0';{'0';{'0';{'0';{'0'}}},...%boundary 1 x=0
{{'0';{'-0.005';{'0';{'0';{'0';{'0'}}}, ...%boundary 2 y=0
{{'0';{'0';{'0';{'0';{'0'}}},...%boundary 3 z=0
{{'0';{'0';{'0';{'0';{'0'}}},...%boundary 4 z=10
{{'0';{'0';{'0';{'0';{'0'}}},...%boundary 5 x=10
{{'0';{'0';{'0';{'0';{'0'}}},...%boundary
{{'0';{'0';{'0';{'0';{'0'}}},...%boundary 7 z=0
{{'0';{'0';{'0';{'0';{'0'}}},...%boundary 8 z=10
{{'0';{'0';{'0';{'0';{'0'}}},...%boundary 9 x=0
{{'0';{'0';{'0';{'0';{'0'}}},...%boundary 11 z=0

```

```

{{'0';{'0';{'0';{'0';{'0'}}},...%boundary 12 z=10
{'-0.005';{'0';{'0';{'0';{'0'}}},...%boundary 13 y=10
{{'0';{'0';{'0';{'0';{'0'}}},...%boundary 16 z=0
{{'0';{'0';{'0';{'0';{'0'}}},...%boundary 17 z=10
{'-0.005';{'0';{'0';{'0';{'0'}}},...%boundary 18 y=0
{'-0.005';{'0';{'0';{'0';{'0'}}},...%boundary 19 y=10
{'-0.005';{'0';{'0';{'0';{'0'}}},...%boundary 22 y=0
{{'0';{'0';{'0';{'0';{'0'}}},...%boundary 24 z=0
{{'0';{'0';{'0';{'0';{'0'}}},...%boundary 25 z=10
{'-0.005';{'0';{'0';{'0';{'0'}}},...%boundary 27 y=10
{{'0';{'0';{'0';{'0';{'0'}}},...%boundary 28 z=0
{{'0';{'0';{'0';{'0';{'0'}}},...%boundary 29 z=10
{{'0';{'0';{'0';{'0';{'0'}}},...%boundary 30 x=10
{{'0';{'0';{'0';{'0';{'0'}}},...%boundary 31 x=10
{{'0';{'0';{'0';{'0';{'0'}}},...%boundary 32 x=10
elseif i==7
bnd.r={{'0';{'0';{'0';{'-100';{'0'}}},...%boundary 1 x=0
{{'0';{'0';{'0';{'0';{'0'}}}, ...%boundary 2 y=0
{{'0';{'0';{'0';{'0';{'0'}}},...%boundary 3 z=0
{{'0';{'0';{'0';{'0';{'0'}}},...%boundary 4 z=10
{{'0';{'0';{'0';{'-100';{'0'}}},...%boundary 5 x=0
{{'0';{'0';{'0';{'0';{'0'}}},...%boundary
{{'0';{'0';{'0';{'0';{'0'}}},...%boundary 7 z=0
{{'0';{'0';{'0';{'0';{'0'}}},...%boundary 8 z=10
{{'0';{'0';{'0';{'-100';{'0'}}},...%boundary 9 x=0
{{'0';{'0';{'0';{'0';{'0'}}},...%boundary 11 z=0
{{'0';{'0';{'0';{'0';{'0'}}},...%boundary 12 z=10
{{'0';{'0';{'0';{'0';{'0'}}},...%boundary 13 y=10
{{'0';{'0';{'0';{'0';{'0'}}},...%boundary 16 z=0
{{'0';{'0';{'0';{'0';{'0'}}},...%boundary 17 z=10
{{'0';{'0';{'0';{'0';{'0'}}},...%boundary 18 y=0
{{'0';{'0';{'0';{'0';{'0'}}},...%boundary 19 y=10
{{'0';{'0';{'0';{'0';{'0'}}},...%boundary 22 y=0
{{'0';{'0';{'0';{'0';{'0'}}},...%boundary 24 z=0
{{'0';{'0';{'0';{'0';{'0'}}},...%boundary 25 z=10
{{'0';{'0';{'0';{'0';{'0'}}},...%boundary 27 y=10
{{'0';{'0';{'0';{'0';{'0'}}},...%boundary 28 z=0
{{'0';{'0';{'0';{'0';{'0'}}},...%boundary 29 z=10
{{'0';{'0';{'0';{'0';{'0'}}},...%boundary 30 x=10
{{'0';{'0';{'0';{'0';{'0'}}},...%boundary 31 x=10
{{'0';{'0';{'0';{'0';{'0'}}},...%boundary 32 x=10
elseif i==8
bnd.r={{'0';{'0';{'0';{'0';{'0'}}},...%boundary 1 x=0
{{'0';{'0';{'0';{'-100';{'0'}}}, ...%boundary 2 y=0
{{'0';{'0';{'0';{'0';{'0'}}},...%boundary 3 z=0
{{'0';{'0';{'0';{'0';{'0'}}},...%boundary 4 z=10
{{'0';{'0';{'0';{'0';{'0'}}},...%boundary 5 x=10
{{'0';{'0';{'0';{'0';{'0'}}},...%boundary
{{'0';{'0';{'0';{'0';{'0'}}},...%boundary 7 z=0
{{'0';{'0';{'0';{'0';{'0'}}},...%boundary 8 z=10
{{'0';{'0';{'0';{'0';{'0'}}},...%boundary 9 x=0
{{'0';{'0';{'0';{'0';{'0'}}},...%boundary 11 z=0
{{'0';{'0';{'0';{'0';{'0'}}},...%boundary 12 z=10

```



```

{{'0';{'0';{'0';{'0';{'0'}}},...%boundary 16 z=0
{{'0';{'0';{'0';{'0';{'0'}}},...%boundary 17 z=0
{{'0';{'0';{'0';{'0';{'0'}}},...%boundary 18 y=0
{{'0';{'0';{'0';{'0';{'0'}}},...%boundary 19 y=10
{{'0';{'0';{'0';{'0';{'0'}}},...%boundary 22 y=0
{{'0';{'0';{'0';{'0';{'0'}}},...%boundary 24 z=0
{{'0';{'0';{'0';{'0';{'0'}}},...%boundary 25 z=10
{{'0';{'0';{'0';{'0';{'0'}}},...%boundary 27 y=10
{{'0';{'0';{'0';{'0';{'0'}}},...%boundary 28 z=0
{{'0';{'0';{'0';{'0';{'0'}}},...%boundary 29 z=10
{{'0';{'0';{'0';{'0';{'0'}}},...%boundary 30 x=10
{{'0';{'0';{'0';{'0';{'0'}}},...%boundary 31 x=10
{{'0';{'0';{'0';{'0';{'0'}}},...%boundary 32 x=10
elseif i==11
  bnd.r={{'0';{'0';{'0';{'0';{'0'}}},...%boundary 1 x=0
    {'0';{'0';{'0';{'0';{'-1'}}}, ...%boundary 2 y=0
    {'0';{'0';{'0';{'0';{'0'}}},...%boundary 3 z=0
    {'0';{'0';{'0';{'0';{'0'}}},...%boundary 4 z=10
    {'0';{'0';{'0';{'0';{'0'}}},...%boundary 5 x=10
    {'0';{'0';{'0';{'0';{'0'}}},...%boundary
    {'0';{'0';{'0';{'0';{'0'}}},...%boundary 7 z=0
    {'0';{'0';{'0';{'0';{'0'}}},...%boundary 8 z=10
    {'0';{'0';{'0';{'0';{'0'}}},...%boundary 9 x=0
    {'0';{'0';{'0';{'0';{'0'}}},...%boundary 11 z=0
    {'0';{'0';{'0';{'0';{'0'}}},...%boundary 12 z=10
    {'0';{'0';{'0';{'0';{'0'}}},...%boundary 13 y=10
    {'0';{'0';{'0';{'0';{'0'}}},...%boundary 16 z=0
    {'0';{'0';{'0';{'0';{'0'}}},...%boundary 17 z=10
    {'0';{'0';{'0';{'0';{'-1'}}},...%boundary 18 y=0
    {'0';{'0';{'0';{'0';{'0'}}},...%boundary 19 y=10
    {'0';{'0';{'0';{'0';{'-1'}}},...%boundary 22 y=0
    {'0';{'0';{'0';{'0';{'0'}}},...%boundary 24 z=0
    {'0';{'0';{'0';{'0';{'0'}}},...%boundary 25 z=10
    {'0';{'0';{'0';{'0';{'0'}}},...%boundary 27 y=10
    {'0';{'0';{'0';{'0';{'0'}}},...%boundary 28 z=0
    {'0';{'0';{'0';{'0';{'0'}}},...%boundary 29 z=10
    {'0';{'0';{'0';{'0';{'0'}}},...%boundary 30 x=10
    {'0';{'0';{'0';{'0';{'0'}}},...%boundary 31 x=10
    {'0';{'0';{'0';{'0';{'0'}}},...%boundary 32 x=10
elseif i==12
  bnd.r={{'0';{'0';{'0';{'0';{'0'}}},...%boundary 1 x=0
    {'0';{'0';{'0';{'0';{'0'}}}, ...%boundary 2 y=0
    {'0';{'0';{'0';{'0';{'-1'}}},...%boundary 3 z=0
    {'0';{'0';{'0';{'0';{'0'}}},...%boundary 4 z=10
    {'0';{'0';{'0';{'0';{'0'}}},...%boundary 5 x=10
    {'0';{'0';{'0';{'0';{'0'}}},...%boundary
    {'0';{'0';{'0';{'0';{'-1'}}},...%boundary 7 z=0
    {'0';{'0';{'0';{'0';{'0'}}},...%boundary 8 z=10
    {'0';{'0';{'0';{'0';{'0'}}},...%boundary 9 x=0
    {'0';{'0';{'0';{'0';{'-1'}}},...%boundary 11 z=0
    {'0';{'0';{'0';{'0';{'0'}}},...%boundary 12 z=10
    {'0';{'0';{'0';{'0';{'0'}}},...%boundary 13 y=10
    {'0';{'0';{'0';{'0';{'-1'}}},...%boundary 16 z=0

```



```

{'0'},...
{'0'};... % end of 1st PDE
{'0','c44p','0','c12p','0','0','0','0'},...
{'c44p','c11p','c44p'},...
{'0','0','0','0','0','c12p','0','c44p','0'},...
{'0'},...
{'0'};... % end of 2nd PDE
{'0','0','c44p','0','0','0','c12p','0','0'},...
{'0','0','0','0','0','c44p','0','c12p','0'},...
{'c44p','c44p','c11p'},...
{'0'},...
{'0'};... % end of 3rd PDE
{'0'},...
{'0'},...
{'0'},...
{'-1'},...
{'0'};... % end of 4th PDE
{'0'},...
{'0'},...
{'0'},...
{'0'},...
{'-1'};... % end of 5th PDE , End of 2nd Group
{'c11m','c16m','c15m','c16m','c66m','c56m','c15m','c56m','c55m'},...
{'c16m','c12m','c14m','c66m','c26m','c46m','c56m','c25m','c45m'},...
{'c15m','c14m','c13m','c56m','c46m','c36m','c55m','c45m','c35m'},...
{'0'},...
{'q11m','q21m','q31m','q16m','q26m','q36m','q15m','q25m','q35m'};...% end of first PDE
{'c16m','c66m','c56m','c12m','c26m','c25m','c14m','c46m','c45m'},...
{'c66m','c26m','c46m','c26m','c22m','c24m','c46m','c24m','c44m'},...
{'c56m','c46m','c36m','c25m','c24m','c23m','c45m','c44m','c34m'},...
{'0'},...
{'q16m','q26m','q36m','q12m','q22m','q32m','q14m','q24m','q34m'};...% end of second PDE
{'c15m','c56m','c55m','c14m','c46m','c45m','c13m','c36m','c35m'},...
{'c56m','c25m','c45m','c46m','c24m','c44m','c36m','c23m','c34m'},...
{'c55m','c45m','c35m','c45m','c44m','c34m','c35m','c34m','c33m'},...
{'0'},...
{'q15m','q25m','q35m','q14m','q24m','q34m','q13m','q23m','q33m'};... % end of thrid PDE
{'0'},...
{'0'},...
{'0'},...
{'-n11m','-n12m','-n13m','-n12m','-n22m','-n23m','-n13m','-n23m','-n33m'},...
{'0'};... % end of 4th PDE
{'q11m','q16m','q15m','q21m','q26m','q25m','q31m','q36m','q35m'},...
{'q16m','q12m','q14m','q26m','q22m','q24m','q36m','q32m','q34m'},...
{'q15m','q14m','q13m','q25m','q24m','q23m','q35m','q34m','q33m'},...
{'0'},...
{'-m11m','-m12m','-m13m','-m12m','-m22m','-m23m','-m13m','-m23m','-m33m'}}; % end of 5th
PDE, end of 3rd Group

```

```

equ.al={{{'0','0','0'},{'0','0','0'},{'0','0','0'},{'0','0','0'},{'0','0','0'},...
'0'},{'0','0','0'},{'0','0','0'},{'0','0','0'},{'0','0','0'},{'0','0','0'},...
{'0','0','0'},{'0','0','0'},{'0','0','0'},{'0','0','0'},{'0','0','0'},{'0','0','0'},...

```



```

fem.appl{1}.equ=equ;

% Internal borders
fem.appl{1}.border='off';

% Shape functions
fem.appl{1}.shape={'shlag(1,"u")','shlag(1,"v")','shlag(1,"w")','shlag(1,"V")','shlag(1,"M")'};

% Geometry element order
fem.appl{1}.sshape=1;

% Define constants
fem.consts={...
    'c11e',C_e(1,1),'c12e',C_e(1,2),'c13e',C_e(1,3),'c14e',C_e(1,4),'c15e',C_e(1,5),'c16e',C_e(1,6),...
    'c22e',C_e(2,2),'c23e',C_e(2,3),'c24e',C_e(2,4),'c25e',C_e(2,5),'c26e',C_e(2,6),...
    'c33e',C_e(3,3),'c34e',C_e(3,4),'c35e',C_e(3,5),'c36e',C_e(3,6),...
    'c44e',C_e(4,4),'c45e',C_e(4,5),'c46e',C_e(4,6),...
    'c55e',C_e(5,5),'c56e',C_e(5,6),...
    'c66e',C_e(6,6),...
...
    'e11e',e_e(1,1),'e12e',e_e(1,2),'e13e',e_e(1,3),'e14e',e_e(1,4),'e15e',e_e(1,5),'e16e',e_e(1,6),...
    'e21e',e_e(2,1),'e22e',e_e(2,2),'e23e',e_e(2,3),'e24e',e_e(2,4),'e25e',e_e(2,5),'e26e',e_e(2,6),...
    'e31e',e_e(3,1),'e32e',e_e(3,2),'e33e',e_e(3,3),'e34e',e_e(3,4),'e35e',e_e(3,5),'e36e',e_e(3,6),...
...
    'n11e',n_e(1,1),'n12e',n_e(1,2),'n13e',n_e(1,3),...
    'n22e',n_e(2,2),'n23e',n_e(2,3),...
    'n33e',n_e(3,3),...
    'm11e',m_e(1,1),'m12e',m_e(1,2),'m13e',m_e(1,3),...
    'm22e',m_e(2,2),'m23e',m_e(2,3),...
    'm33e',m_e(3,3),...
...
    'c11m',C_m(1,1),'c12m',C_m(1,2),'c13m',C_m(1,3),'c14m',C_m(1,4),'c15m',C_m(1,5),'c16m',C_m(1,6),...
    'c22m',C_m(2,2),'c23m',C_m(2,3),'c24m',C_m(2,4),'c25m',C_m(2,5),'c26m',C_m(2,6),...
    'c33m',C_m(3,3),'c34m',C_m(3,4),'c35m',C_m(3,5),'c36m',C_m(3,6),...
    'c44m',C_m(4,4),'c45m',C_m(4,5),'c46m',C_m(4,6),...
    'c55m',C_m(5,5),'c56m',C_m(5,6),...
    'c66m',C_m(6,6),...
...
    'q11m',q_m(1,1),'q12m',q_m(1,2),'q13m',q_m(1,3),'q14m',q_m(1,4),'q15m',q_m(1,5),'q16m',q_m(1,6),...
    'q21m',q_m(2,1),'q22m',q_m(2,2),'q23m',q_m(2,3),'q24m',q_m(2,4),'q25m',q_m(2,5),'q26m',q_m(2,6),...
    'q31m',q_m(3,1),'q32m',q_m(3,2),'q33m',q_m(3,3),'q34m',q_m(3,4),'q35m',q_m(3,5),'q36m',q_m(3,6),...
...
    'n11m',n_m(1,1),'n12m',n_m(1,2),'n13m',n_m(1,3),...
    'n22m',n_m(2,2),'n23m',n_m(2,3),...
    'n33m',n_m(3,3),...

```

```

'm11m',m_m(1,1),'m12m',m_m(1,2),'m13m',m_m(1,3),...
    'm22m',m_m(2,2),'m23m',m_m(2,3),...
    'm33m',m_m(3,3),...
...
'c11p', mult*0.55328,...
'c12p', mult*0.29792,...
'c44p', mult*0.12768};

% Multiphysics
fem=multiphysics(fem);

% Extend the mesh
fem.xmesh=meshextend(fem,'context','local','cplbndeq','on','cplbndsh','on');

% Evaluate initial condition
init=assemnit(fem,...
    'context','local',...
    'init', fem.xmesh.elemnit);

if z==1
% Solve problem using normal solver
fem.sol=femlin(fem,...
    'jacobian','numeric',...
    'out', {'sol'},...
    'init', init,...
    'context','local',...
    'sd', 'off',...
    'nullfun','flspnull',...
    'blocksize',5000,...
    'solcomp',{'M','V','u','v','w'},...
    'linsolver','matlab',...
    'method','lagrange',...
    'uscale','auto');
elseif z==2
% Solve problem iterative
fem.sol=femiter(fem,...
    'init', init,...
    'nonlin','off',...
    'out', 'sol',...
    'report','on',...
    'stop', 'on',...
    'context','local',...
    'sd', 'off',...
    'nullfun','fnullorth',...
    'blocksize',5000,...
    'solcomp',{'M','V','u','v','w'},...
    'method','eliminate',...
    'uscale','auto',...
    'itrestart',10,...
    'itsolv','gbit',...
    'maxlinit',3000,...
    'prefun','luinc',...
    'itol', 10e-09,...

```

```

        'rhob', 40,...
        'prepar', struct('droptol',{0.00001},'thresh',{1},'milu',{1},'udiag',{1}, ...
'preorder',{1}));
end

% Save current fem structure for restart purposes
fem0=fem;

% Integrate on subdomains
I(1,i)=postint(fem,'ux',...
    'cont', 'off',...
    'contorder',2,...
    'edim', 3,...
    'solnum', 1,...
    'phase', 0,...
    'geomnum',1,...
    'dl', [1 2 3 4 5 6],...
    'intorder',4,...
    'context','local');
I(2,i)=postint(fem,'vy',...
    'cont', 'off',...
    'contorder',2,...
    'edim', 3,...
    'solnum', 1,...
    'phase', 0,...
    'geomnum',1,...
    'dl', [1 2 3 4 5 6],...
    'intorder',4,...
    'context','local');
I(3,i)=postint(fem,'wz',...
    'cont', 'off',...
    'contorder',2,...
    'edim', 3,...
    'solnum', 1,...
    'phase', 0,...
    'geomnum',1,...
    'dl', [1 2 3 4 5 6],...
    'intorder',4,...
    'context','local');
I(4,i)=postint(fem,'vz',...
    'cont', 'off',...
    'contorder',2,...
    'edim', 3,...
    'solnum', 1,...
    'phase', 0,...
    'geomnum',1,...
    'dl', [1 2 3 4 5 6],...
    'intorder',4,...
    'context','local');
I(5,i)=postint(fem,'wx',...
    'cont', 'off',...
    'contorder',2,...
    'edim', 3,...

```

```

'solnum', 1,...
'phase', 0,...
'geomnum', 1,...
'dl', [1 2 3 4 5 6],...
'intorder', 4,...
'context', 'local');
I(6,i)=postint(fem,'uy',...
'cont', 'off',...
'contorder', 2,...
'edim', 3,...
'solnum', 1,...
'phase', 0,...
'geomnum', 1,...
'dl', [1 2 3 4 5 6],...
'intorder', 4,...
'context', 'local');
I(7,i)=postint(fem,'Vx',...
'cont', 'off',...
'contorder', 2,...
'edim', 3,...
'solnum', 1,...
'phase', 0,...
'geomnum', 1,...
'dl', [1 2 3 4 5 6],...
'intorder', 4,...
'context', 'local');
I(8,i)=postint(fem,'Vy',...
'cont', 'off',...
'contorder', 2,...
'edim', 3,...
'solnum', 1,...
'phase', 0,...
'geomnum', 1,...
'dl', [1 2 3 4 5 6],...
'intorder', 4,...
'context', 'local');
I(9,i)=postint(fem,'Vz',...
'cont', 'off',...
'contorder', 2,...
'edim', 3,...
'solnum', 1,...
'phase', 0,...
'geomnum', 1,...
'dl', [1 2 3 4 5 6],...
'intorder', 4,...
'context', 'local');
I(10,i)=postint(fem,'Mx',...
'cont', 'off',...
'contorder', 2,...
'edim', 3,...
'solnum', 1,...
'phase', 0,...
'geomnum', 1,...

```

```

'dl', [1 2 3 4 5 6],...
'intorder',4,...
'context','local');
I(11,i)=postint(fem,'My',...
'cont', 'off',...
'contorder',2,...
'edim', 3,...
'solnum', 1,...
'phase', 0,...
'geomnum',1,...
'dl', [1 2 3 4 5 6],...
'intorder',4,...
'context','local');
I(12,i)=postint(fem,'Mz',...
'cont', 'off',...
'contorder',2,...
'edim', 3,...
'solnum', 1,...
'phase', 0,...
'geomnum',1,...
'dl', [1 2 3 4 5 6],...
'intorder',4,...
'context','local');

% O matrix
O(1,i)=postint(fem,'cu1x',...
'cont', 'off',...
'contorder',2,...
'edim', 3,...
'solnum', 1,...
'phase', 0,...
'geomnum',1,...
'dl', [1 2 3 4 5 6],...
'intorder',4,...
'context','local');
O(2,i)=postint(fem,'cu2y',...
'cont', 'off',...
'contorder',2,...
'edim', 3,...
'solnum', 1,...
'phase', 0,...
'geomnum',1,...
'dl', [1 2 3 4 5 6],...
'intorder',4,...
'context','local');
O(3,i)=postint(fem,'cu3z',...
'cont', 'off',...
'contorder',2,...
'edim', 3,...
'solnum', 1,...
'phase', 0,...
'geomnum',1,...
'dl', [1 2 3 4 5 6],...

```

```

'intorder',4,...
'context','local');
O(4,i)=postint(fem,'cu2z',...
'cont', 'off',...
'contorder',2,...
'edim', 3,...
'solnum', 1,...
'phase', 0,...
'geomnum',1,...
'dl', [1 2 3 4 5 6],...
'intorder',4,...
'context','local');
O(5,i)=postint(fem,'cu3x',...
'cont', 'off',...
'contorder',2,...
'edim', 3,...
'solnum', 1,...
'phase', 0,...
'geomnum',1,...
'dl', [1 2 3 4 5 6],...
'intorder',4,...
'context','local');
O(6,i)=postint(fem,'cu1y',...
'cont', 'off',...
'contorder',2,...
'edim', 3,...
'solnum', 1,...
'phase', 0,...
'geomnum',1,...
'dl', [1 2 3 4 5 6],...
'intorder',4,...
'context','local');
O(7,i)=postint(fem,'cu4x',...
'cont', 'off',...
'contorder',2,...
'edim', 3,...
'solnum', 1,...
'phase', 0,...
'geomnum',1,...
'dl', [1 2 3 4 5 6],...
'intorder',4,...
'context','local');
O(8,i)=postint(fem,'cu4y',...
'cont', 'off',...
'contorder',2,...
'edim', 3,...
'solnum', 1,...
'phase', 0,...
'geomnum',1,...
'dl', [1 2 3 4 5 6],...
'intorder',4,...
'context','local');
O(9,i)=postint(fem,'cu4z',...

```



```

    'cont', 'off',...
    'contorder',2,...
    'edim', 3,...
    'solnum', 1,...
    'phase', 0,...
    'geomnum',1,...
    'dl', [1 2 3 4 5 6],...
    'intorder',4,...
    'context','local');
O(10,i)=postint(fem,'cu5x',...
    'cont', 'off',...
    'contorder',2,...
    'edim', 3,...
    'solnum', 1,...
    'phase', 0,...
    'geomnum',1,...
    'dl', [1 2 3 4 5 6],...
    'intorder',4,...
    'context','local');
O(11,i)=postint(fem,'cu5y',...
    'cont', 'off',...
    'contorder',2,...
    'edim', 3,...
    'solnum', 1,...
    'phase', 0,...
    'geomnum',1,...
    'dl', [1 2 3 4 5 6],...
    'intorder',4,...
    'context','local');
O(12,i)=postint(fem,'cu5z',...
    'cont', 'off',...
    'contorder',2,...
    'edim', 3,...
    'solnum', 1,...
    'phase', 0,...
    'geomnum',1,...
    'dl', [1 2 3 4 5 6],...
    'intorder',4,...
    'context','local');
endtime=fix(clock)
etime(clock,t0)/60
end

%%%%%%%%%%
% Mori-Tanaka Method
%%%%%%%%%%

% piezomagnetic material tensor
E_1=[C_m,zeros(6,3),q_m';zeros(3,6),-n_m,zeros(3,3);q_m,zeros(3,3),-m_m];

% piezoelectric material tensor
E_2=[C_e,e_e',zeros(6,3);e_e,-n_e,zeros(3,3);zeros(3,6),zeros(3,3),-m_e];
%Material Properties

```

```

%matrix(m)Epoxy
c11_m=mult*0.55328;
c12_m=mult*0.29792;
c44_m=mult*0.12768;
nu_m=0.35;

%Stiffness matrix for transversely isotropic materials
% Lm Stiffnes of Matix
E_m=zeros(12,12);
E_m(1,1)=c11_m;E_m(1,2)=c12_m;E_m(1,3)=c12_m;
E_m(2,1)=c12_m;E_m(2,2)=c11_m;E_m(2,3)=c12_m;
E_m(3,1)=c12_m;E_m(3,2)=c12_m;E_m(3,3)=c11_m;
E_m(4,4)=c44_m;
E_m(5,5)=c44_m;
E_m(6,6)=c44_m;
E_m(7,7)=-1;E_m(8,8)=-1;E_m(9,9)=-1;E_m(10,10)=-1;E_m(11,11)=-1;E_m(12,12)=-1;

ID=eye(12,12);
%for cylindrical fiber

%Eshelby tensor for isotropic matrices and cylindrical inclusion
nu=nu_m;
es=zeros(12,12);
es(1,1)=(5-4*nu)/8/(1-nu);es(1,2)=(4*nu-1)/8/(1-nu);es(1,3)=nu/2/(1-nu);
es(2,1)=(4*nu-1)/8/(1-nu);es(2,2)=(5-4*nu)/8/(1-nu);es(2,3)=nu/2/(1-nu);
es(4,4)=1/2;
es(5,5)=1/2;
es(6,6)=2*(3-4*nu)/8/(1-nu);
es(7,7)=1/2;
es(8,8)=1/2;
es(10,10)=1/2;
es(11,11)=1/2;

cm=1-V1/100-V2/100;c1=V1/100;

A_d1=inv(ID+es*inv(E_m)*(E_1-E_m));
A_d2=inv(ID+es*inv(E_m)*(E_2-E_m));

A_mt1=A_d1*inv(cm*ID+c1*A_d1+(1-c1-cm)*A_d2);
A_mt2=A_d2*inv(cm*ID+c1*A_d1+(1-c1-cm)*A_d2);

E_mt=E_m+c1*(E_1-E_m)*A_mt1+(1-c1-cm)*(E_2-E_m)*A_mt2;

K=O*inv(I);
I(:,7:9)=I(:,7:9)/10000;
I(:,10:12)=I(:,10:12)/100;
O(:,7:9)=O(:,7:9)/10000;
O(:,10:12)=O(:,10:12)/100;
I
O
K

```


VITA

Jae Sang Lee

Permanent address

289-33 Nock-Won A.P.T. 101-1203

Eunhang-Dong, Syheung-Si,

Kyong-Ki-Do, Korea 429-836

Personal

Date of birth: March 6, 1974

Place of birth: Seoul, Korea

Education

M.S. Aerospace Engineering (December 2003)
Texas A&M University, College Station, TX.

B.S. Aerospace Engineering (February 1998)
Seoul National University, Seoul, Korea.

Professional Experience

Graduate Research Assistant (Jan. 2003 ~ Sep. 2003)

SMART Research Group, Texas A&M University, College Station, TX.

MRB Engineer (Jul. 1998 ~ Jul. 2001)

Design Group, Structural Engineering Section, Engineering
Team, Aerospace Division, Korean Air